NASA Technical Memorandum 100678

In-Orbit Calibration Adjustment of the Nimbus-7 SMMR

Per Gloersen
Goddard Space Flight Center
Greenbelt, Maryland

National Aeronautics
and Space Administration

**Scientific and Technical
Information Branch**

1987

CONTENTS

IN-ORBIT CALIBRATION ADJUSTMENT OF THE NIMBUS-7 SMMR

1. INTRODUCTION

Prior to its launch on October 24, 1978, the Nimbus-7 Scanning Multichannel Microwave Radiometer (SMMR) was tested in a thermal-vacuum chamber at the Jet Propulsion Laboratory. One of the tests was to measure the response of each of the ten SMMR channels (Gloersen & Barath, 1977) to a black-body target operated at a variety of temperatures ranging from 77 K to 320 K, as was also done for the SMMR on board the SeaSat (Njoku, 1980). These responses formed the basis for a so-called prelaunch calibration of the instrument. In addition, antenna pattern measurements were made for the purpose of determining actual performance beam-widths and are used here to determine the fraction of the beam directed over the horizon into space. Losses over some of the waveguide runs between the antenna and radiometers were also measured. These measurements, and a semi-empirical correction for the observed polarization mixing (Gloersen et al., 1980) were used to prepare one of the archival radiance products called the CELL tapes (Gloersen et al., 1984), which are integrated field-of-view (IFOV) data remapped into cells approximately a beam-width in extent.

The rationale behind the CELL tape approach is that in order to use multispectral radiances to calculate geophysical parameters such as sea surface temperatures (SSTs), all SMMR channels should be mapped into cells of equivalent size prior to calculation. This also reduces radiometer noise. A disadvantage of this scheme is that inherent spatial resolution available as a result of oversampling of the IFOVs is lost when remapping into the cells as prescribed. An alternate archival product has been developed which takes the basic raw count data stored for each IFOV on tapes called TATs and produces radiances stored in exactly the same format as the TATs but with only a minimal loss in resolution resulting from the polarization mixing correction. These latter tapes are called TCTs. In addition, the TCTs include a calibration adjustment. A comparison of the salient features of the CELL and TCT tapes is given in Table 1.

During the course of developing the semi-empirical correction for polarization mixing (Gloersen et al., 1980, Gloersen, 1983), analysis of the data showed that several independent means for determining radiance differences between the two polarizations for each of the five wavelengths yielded discrepancies and pointed to polarization leakages between the horizontal (H) and vertical (V) channels in addition to the mixing by antenna rotation. These observations were supported by model calculations of the radiance differences in the H and V channels, which did not agree with the observations. Before launch, individual components were tested for cross-polarization leakage, but the integrated system was not adequately checked due to launch schedule pressures and funding limitations. Such leakage was not taken into account in the calibration of the CELL tapes. It was decided to take these discrepancies into account when developing the calibration procedure for the TCTs described below.

Since the prelaunch tests confirmed the expected linearity of the SMMR electronics, the TCT calibration adjustment scheme is based on selection of two tiepoints. The tiepoint at the warm end of the radiance scale is the internal warm reference adjusted for the portion of the beam spilling over the horizon into space. This adjustment is necessary so that when the SMMR is used to observe the radiance from an earth target at the same brightness temperature as the physical temperature of the warm reference, the observed signal is not too low because of the space spillover effect. The cold tiepoint is a zonal area of the global oceans selected, among other things, for low spatial variation in climatological SSTs, so as to reduce the errors in the model calculations of the oceanic zone. For this tiepoint, taking the space spillover fraction into account is inherent in adjusting the observed signal to correspond to the modeled oceanic radiances. Two sets of calculated radiances were used for the oceanic zone; one representing the average climatological values of near-surface winds (NSWs), water vapor, and clouds for comparison with the results from the polarization analysis; and another one with minimum values of these parameters for comparison with minimum radiances observed in the zone.

As indicated in Table 1, the TCT calibration process proceeds in three steps. The several elements in Step 1 are discussed in Sections 2 and 3. A polarization mixing correction is described in Section 4. Some of the results from Section 4 are used in the adjustment scheme. Steps 2 and 3 are described in Section 5. The ocean/atmosphere radiative transfer model used to provide the cold tiepoint for the calibration adjustment is described in Appendix A and a BASIC program implementation of this model is listed in Appendix B.

Table 1. Comparison of CELL and TCT Tape Characteristics

Property	CELL Tape	TCT Tape
Integrated FOV	Rectangular	Round
4.6 cm	156 X 158 km	148 X 148 km
1.7 cm	97.5 X 98.5 km	91 X 91 km
1.4 cm	60 X 60.6 km	46 X 46 km
0.8 cm	30 X 30.3 km	27 X 27 km
Cross-track sampling interval		
4.6 cm	156 km	56 km (av.)
2.8 cm	97.5 km	26 km (av.)
1.7 cm	60 km	26 km (av.)
1.4 cm	60 km	26 km (av.)
0.8 cm	30 km	13 km (av.)
Along-track sampling interval		
4.6 cm	158 km	26 km
2.7 cm	98.5 km	26 km
1.7 cm	60.6 km	26 km
1.4 cm	60.6 km	26 km
0.8 cm	30.3 km	13 km
Calibration Technique	Regression fit to five-step BB calibration target at five different instrument temperatures. (Prelaunch calibration). Temperature gradient terms added.	Step 1: Prelaunch calibration. Step 2: Correction of offset and gain factors in prelaunch calibration using modeled radiances. Step 3: Second-order adjustment to offset and gain factors using modeled minimum radiances.
Antenna Pattern Correction	Takes into account both space spillover and contributions from adjacent cells.	Uses space spillover fraction only.
Sun in Cold Horn	Cold counts held constant over wide solar acquisition window, corresponding to sun declination angle range of 80 degrees. This results in a 2 K radiance jump in the 4.6 cm channels.	Cold counts are linearly interpolated within narrower moving solar acquisition window thus avoiding radiance jumps.

2. PRELAUNCH CALIBRATION

An initial calibration of the Nimbus-7 SMMR was carried out in a thermal-vacuum chamber (TVC) at the Jet Propulsion Laboratory (JPL) during the course of system tests on the instrument. Details of this and other tests are contained in the contractor's report (not published) delivered to Goddard by JPL. Similar tests on the Seasat SMMR have also been described by Njoku, et al., (1980). Briefly, the SMMR was used to record ten-channel microwave radiances while viewing a nearly black-body target held at a number of temperature levels ranging from 77 K to 320 K, and while varying the SMMR instrument temperature over a range somewhat beyond the anticipated operating range onboard the satellite. The data were subjected to both linear and second-order regression analyses in order to provide a formula to compute brightness temperatures (radiances) from the digitized signals (counts) from the SMMR. Within the observed radiometer switch temperature range (+/− 2 K) onboard the satellite, there is no perceptable difference (less than 0.1 K on all channels) between the results from using either the linear or quadratic regression coefficients in this calculation. The linear set was chosen for the CELL calibration. The quadratic set, which had a better fit outside this normal operating range, was adopted for the TCT tapes in the unlikely event that the satellite ambient temperature range should change. It should also be noted that the CELL calibration includes correction terms for some of the temperature gradients along the waveguide run between the antenna and the radiometers. Since these correction terms utilized incomplete component loss measurements made prior to assembly and are therefore of questionable value, they are not included in the TCT calibration.

The form of the equation used in the regression analysis is as follows:

$$TB = a0 + a1*th + a3*(th-th0)^2 + [a2*(tc-th) + a4*(th-th0)^2]*N \quad (1)$$

where

th is the temperature of the radiometer's Dicke switch

th0 is a mid-range value of th (based on predicted orbital values)

tc is the radiance from a liquid nitrogen-cooled target (77 K) during the TVC tests and from outer space (2.7 K) after launch

N = (TA−TH)/(TC−TH) is the normalized signal (counts), and where

TA is the radiometric signal from the SMMR antenna

TH is the radiometric signal from the warm reference

TC is the radiometric signal from the cold reference

There are ten sets of these coefficients, one for each channel. However, they are of little consequence for the present discussion since they provide only a temporary calibration level for the TCT-format data. The ten equations (Eq. 1), one for each SMMR channel, are used to convert the radiometer counts stored on the TATs into interim radiances, which are used in the subsequent polarization mixing correction procedure.

3. SPACE SPILLOVER FRACTIONS

The antenna portion of the SMMR was tested on an antenna range as part of the prelaunch testing carried out by JPL. JPL was requested (J. Stacey, priv. comm.) to analyze the antenna patterns and calculate the space spillover fraction (the fraction of the beam passing over the horizon into space, SF) for each channel. The results are shown in Table 2.

These fractions are used in adjusting the brightness temperature of the warm load to an equivalent radiance, such that when a target with a brightness temperature equal to the physical temperature of the warm reference is observed, the radiometer will not indicate too low a radiance due to the beam spillover into space. Within the radiometer, this corresponds to the normalized counts, N, being equal to zero, e.g., TA = TH (see Equation 1).

Table 2. Fraction of Antenna Beam Viewing Space (SF)

Wavelength (cm)	4.6	2.7	1.7	1.4	0.81
H Polarization	0.049646	0.034773	0.021596	0.022840	0.010807
V Polarization	0.065527	0.040192	0.022590	0.023250	0.013304

4. ANALYSIS OF THE POLARIZATION DATA OBTAINED IN ORBIT

During the prelaunch testing of SMMR on the antenna range, neither the actual radiometers nor the microwave switches used to change from H to V polarization and from the antenna to the reference signals were part of this test, due to the impracticality of using the radiometers as receivers for the antenna range sources. This was unfortunate in that knowledge of the cross-channel polarization leakage was not obtained. Testing of leakage in the individual microwave switches was carried out, but the results from these tests were insufficient to predict the apparent leakages observed in orbit.

In order to arrive at a suitable polarization mixing correction scheme, SMMR data on TATs were first calibrated with the prelaunch coefficients. Then, oceanic radiances were averaged into each IFOV for every ten degrees of latitude, separated into daytime and nighttime sets, for one month's data for November 1978, December 1978, March 1979, and June 1979. Details of these observations are described elsewhere (Gloersen et al., 1980, Gloersen, 1983). A subset of these observations was used here for the purposes of adjusting the calibration.

The procedure consisted of fitting the averaged interim global oceanic radiances in each IFOV to the following functions of the scan angle, A:

$$P = P0 + P1*\cos(2*A) + P2*\sin(2*A)$$

$$S = S0 + S1*\cos(2*A) + S2*\sin(2*A) \qquad (2)$$

where P and S are the signals directly from the 'horizontal' and 'vertical' channels of the SMMR, respectively. Multiple linear regression with the variables cos(2*A) and sin(2*A) was used to fit the P and S interim global oceanic radiance data for each oceanic zone (sufficiently far from shorelines), and to obtain the regression coefficients, Pi, Si in Equation (2) for the time periods and zones already listed. Examples of such fits are shown in Figures 1-5 (from Gloersen et al., 1980). The standard deviation of the fit was less than 0.5 K in this entire data set, and less than 0.2 K for the December 1978 daytime set. Within the latter set, the standard deviation was consistently less for the 30S-40S latitude zone, and so those data were selected for the calibration adjustment coefficients.

Equation (2) may be rewritten as:

$$P = Pmin + Rh*[\sin(A - Dh)]^2$$

$$S = Smax - Rv*[\sin(A - Dv)]^2 \qquad (3)$$

where $Pmin = P0 - Rh/2$

$$Smax = S0 + Rv/2$$

$$Rh = 2*\mathrm{sqrt}(P1^2 + P2^2)$$

$$Rv = 2*\mathrm{sqrt}(S1^2 + S2^2)$$

$$Dh = 0.5*\arctan(P2/P1)$$

$$Dv = 0.5*\arctan(S2/S1)$$

The polarization mixing correction equations developed from this analysis are discussed in detail elsewhere (Gloersen, 1983) but are also given here. Designating the corrected values for the horizontal and vertical channels as HP and VS, respectively,

$$HP = P - (S - P)*BP/(AP - BP*Rv/Rh)$$

$$VS = S + (S - P)*BS/(AS - BS*Rh/Rv) \qquad (4)$$

where $BP = \sin^2(A - Dh)$

$$BS = \sin^2(A - Dv)$$

$$AP = (Smax - Pmin)/Rh$$

$$AS = (Smax - Pmin)/Rv$$

Values for these coefficients are given in Table 3.

In the formulation of Equation (3), Rh and Rv may be visualized as magnitudes of rotating vectors. When the phase angle is 90 degrees, Rh and Rv ideally convert P to S and S to P, respectively. Thus, ideally (i.e., if there are no leakages between P and S channels in the switches, the multifrequency horn, or the antenna dish structure), Rh, Rv, and (Smax − Pmin) should all be equal, presuming the calibrations are correct. In addition, the phase angles, Dh and Dv, should be zero. As can be seen in Table 3, such is not the case.

Based on these results, either the prelaunch calibration targets were poor black-bodies or there is substantial cross-polarization leakage between the SMMR H & V channels, which could not be discerned with black-body calibration targets. The additional observation that the phase shift angles, Dh and Dv, are non-zero (Table 3) supports the latter conclusion. (The differences in the space spillover factors [see Table 2] between the polarization channels at a given wavelength were at most, 1.6%, and so are too small to account for the observed discrepancies.) It is interesting to note that the larger the phase shift difference in the H and V channels of a given wavelength, the smaller the radiance difference, Smax − Pmin.

Finally, model calculations of H, V, and (V − H) (Table 3) predict radiances of the H and V channels as

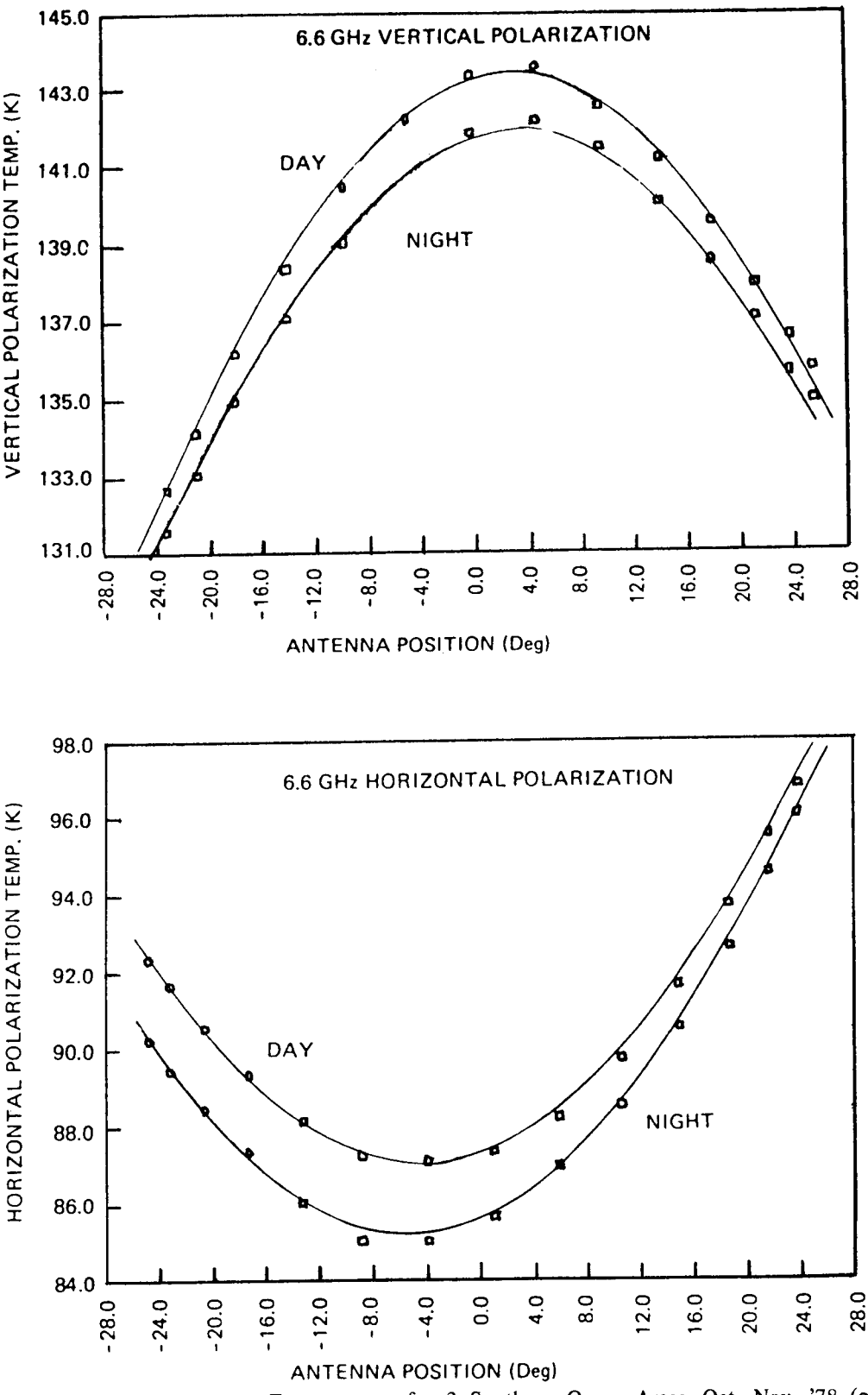

SMMR Ave. Uncorrected Antenna Temperatures for 3 Southern Ocean Areas–Oct, Nov, '78 (~340 Orb)

Figure 1.

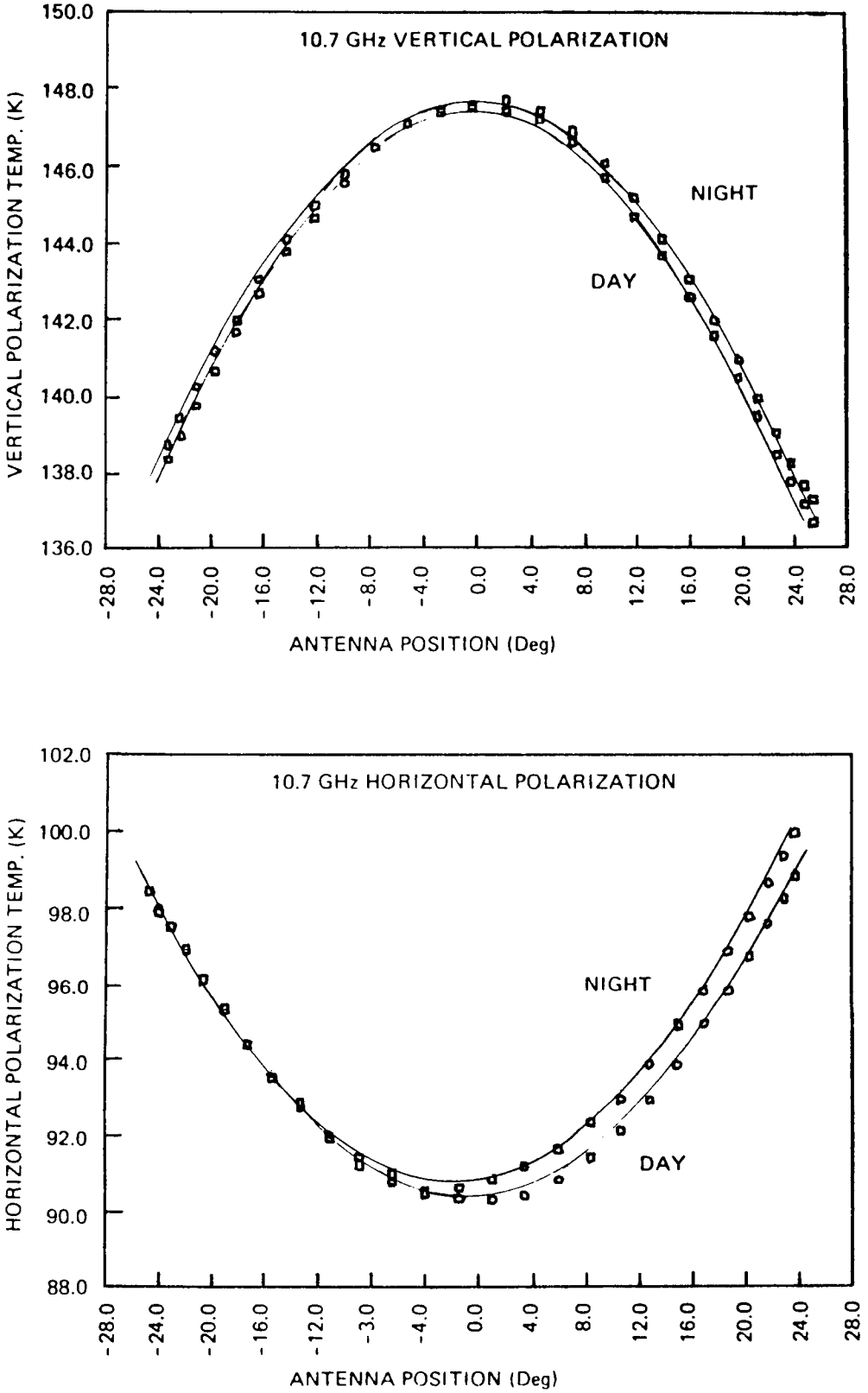

SMMR Ave. Uncorrected Antenna Temperatures for 3 Southern Ocean Areas–Oct, Nov, '78 (~340 Orb)

Figure 2.

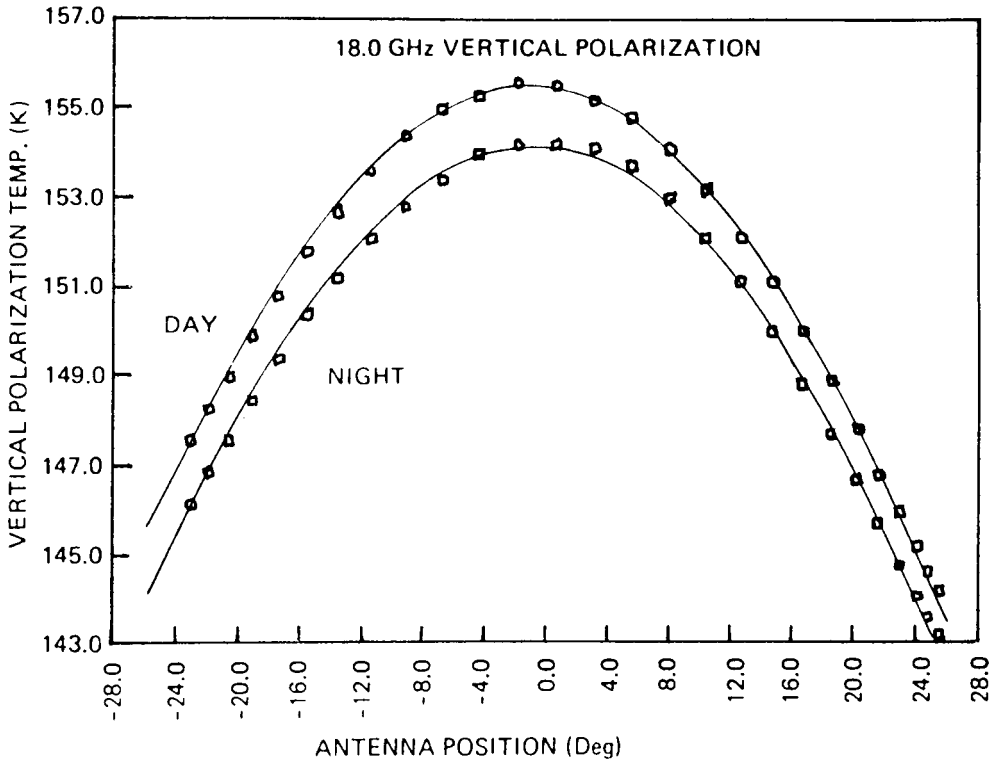

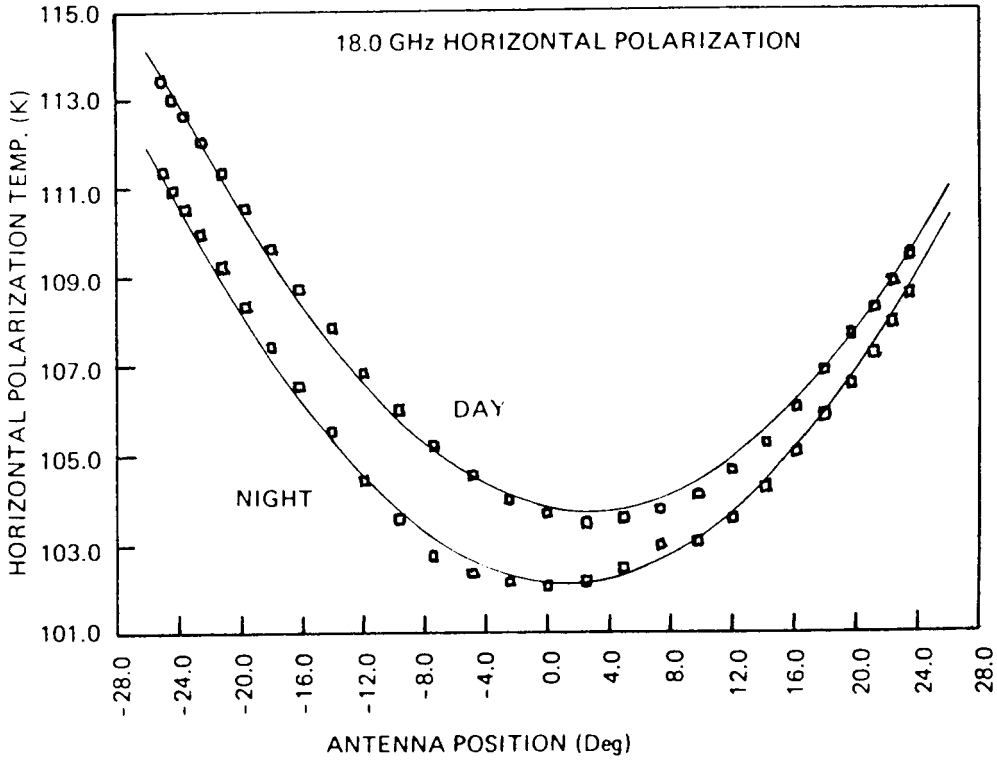

SMMR Ave. Uncorrected Antenna Temperatures for 3 Southern Ocean Areas–Oct, Nov, '78 (~340 Orb)

Figure 3.

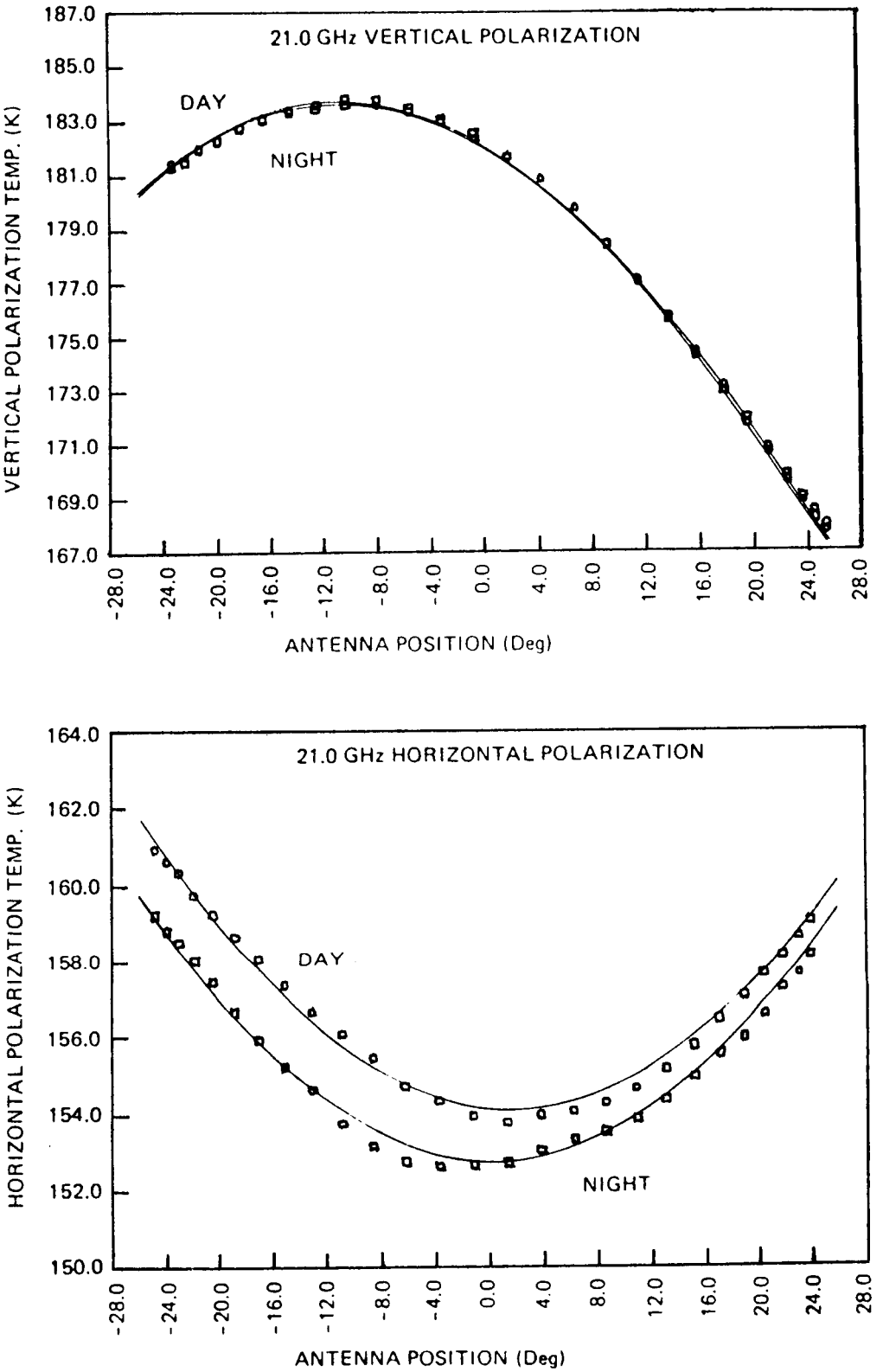

SMMR Ave. Uncorrected Antenna Temperatures for 3 Southern Ocean Areas–Oct, Nov, '78 (~340 Orb)

Figure 4.

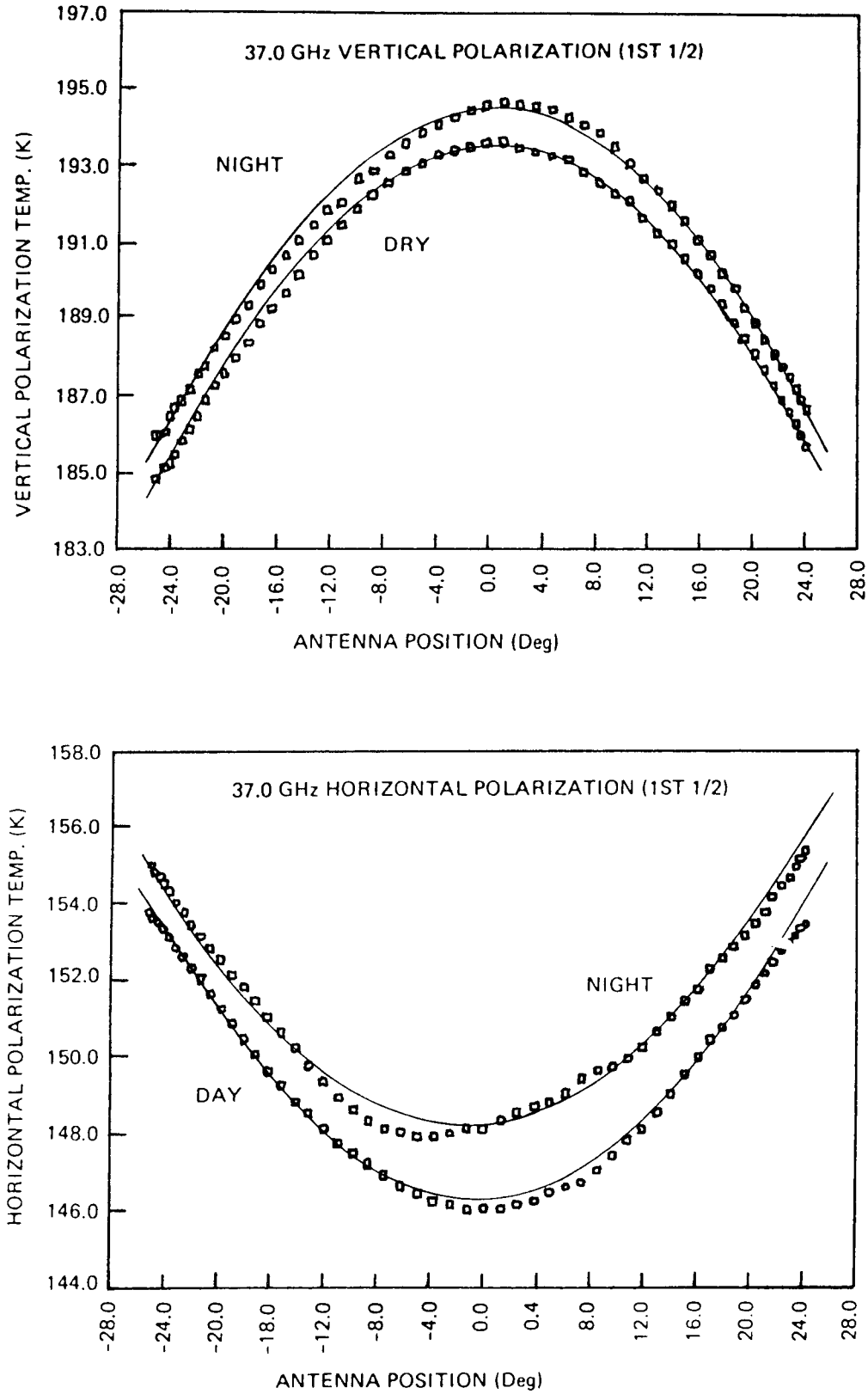

SMMR Ave. Uncorrected Antenna Temperatures for 3 Southern Ocean Areas–Oct, Nov, '78 (~340 Orb)

Figure 5.

much as 15 K higher and polarization differences as much as 17 K higher than the corresponding Pmin, Smax, and (Smax – Pmin) inferred from this polarization analysis. With calibration discrepancies of this magnitude, comparisons of observed radiances with model calculations or instruments with better calibrations would be puzzling, to say the least.

Table 3. Regression Coefficients.

	Wavelength (cm)				
	4.6	2.8	1.7	1.4	0.81
Dh (degrees)	4.7	1.5	-2.4	-3.6	0.7
Dv (degrees)	(-1.9 to -3.8)*	(-0.1 to +1.0)*	1.4	10.8	-0.2
Pmin (kelvins)	83.3	88.7	109.7	146.8	140.8
H (model)**	90.0	97.6	111.5	137.6	139.4
Smax (kelvins)	138.2	147.4	161.8	183.5	193.1
V (model)**	153.9	159.2	172.9	191.1	200.9
Rh (kelvins)	51.0	54.0	49.8	42.8	46.3
Rv (kelvins)	58.1	61.3	57.1	49.2	51.5
Smax - Pmin	54.9	58.7	52.1	36.6	62.6
(V-H) (model)**	63.9	61.6	61.4	53.5	61.5

*Varies predictably with latitude
**Appendix A

5. CALIBRATION ADJUSTMENT PROCEDURE

In view of the foregoing, it was decided to adjust the calibration of the SMMR to agree with model calculations with as few atmosphere and wind contributions as possible. The model used for these purposes is described in Appendix A. Based on the linear response of the SMMR amplifiers observed in the prelaunch tests, a two-point recalibration scheme was adopted. The warm calibration point was obtained by using the physical temperature of the internal warm reference (a waveguide termination load inside the radiometer box) adjusted by a factor utilizing the space spillover factor. The cold reference consisted of model calculations of the radiation from the global ocean zone, as mentioned earlier.

The equations used in both stages of the calibration adjustment follow. Redefining the coefficients in Equation (1),

$$A(th) = a0 + a1*th + a3*(th - t0)^2$$

$$B(th) = a2*(tc - th) + a4*(th - th0)^2 \quad (5)$$

where tc = 77 K in the thermal vacuum chamber

= 2.7 K in orbit.

Combining Equations (1) and (5),

$$TB = A(th) + B(th)*N \quad (6)$$

The corrected radiances, TB', are calculated from TB with the use of offset (a) and gain (b) correction factors, to be determined below, as follows:

$$TB' = a + b*TB = A' + B'*N \quad (7)$$

Solving Equations (6) and (7) simultaneously,

$$A' = a + b*A$$

$$B' = b*B \quad (8)$$

The factors a and b are obtained from simultaneously solving the following two equations, which represent the cold and warm tiepoints, respectively:

$$TBm = a + b*TBo$$

$$A' = a + b*A \quad (9)$$

where TBm is the model oceanic radiance for either H or V and TBo is either Pmin or Smax for each of the five wavelengths. A' is simply A corrected for the space spillover fraction, SF, (see Section 3) as follows:

$$A' = (A - 2.7*SF)/(1 - SF) \quad (10)$$

Note that when N = 0 (Equation 7), TB' = A'. The resulting correction factors, a and b, are then

$$a = TBm - b*TBo$$

$$b = (TBm - A')/(TBo - A) \quad (11)$$

Since the polarization analysis by its nature used oceanic data with averaged oceanic radiances, for which the model calculations are less reliable, it was necessary to calculate two different sets of ocean surface tiepoints. First, model calculations for the average ocean surface characteristics in the global zone 30-40°S for December 1978, (see Figure 6) were used to compare with the polarization mixing measurements described in the previous section. The zonally averaged ocean/atmosphere conditions assumed for this calculation were SST = 290.4 K, NSW = 7 m/s, average tropospheric temperature = 278.3 K, cloud water in the column = 0, and water vapor = 1.6 cm, all based on climatological values for average conditions from the U.S. Navy Climatic Atlas of the World (NAVAIR 50-1C-54, 1969).

Next, the values of Pmin and Smax were used in Equations (11) to obtain a preliminary set of values for a and b. Radiances obtained with this preliminary set of a and b were then used in the polarization correction algorithm to produce interim TCTs for the December 1978 test period. These, in turn, were used to produce radiance histograms of each channel (see Figures 7-16). It was surmised that the minimum radiances for each channel obtained from the histograms corresponded to milder atmospheric conditions than before; i.e., NSW = 0 and water vapor = 1.0 cm, based this time on the minimum climatological values. The assumption of zero winds also served to minimize the change in surface emissivity with NSW.

The radiance differences (called 'adjustments') between model calculations using milder weather conditions and minimum values obtained from histograms are given in Table 4.

These differences are interpreted as errors in the model calculations for the global oceanic zonal averages of the TBm's used in Equation (11). Thus, they were used to adjust the cold tiepoints, TBm, and Equations (11) were again utilized to obtain final values for a and b. The results are tabulated in Table 5.

Also shown in Table 5 are values of a' and b' which are intercept and slope adjustments used to translate between TCTs and CELLs, obtained from a comparison of values in the north polar region (see Figures 17-26). Figures 17-26 also illustrate the comparison between CELL radiances and the model calculations (the TCT values).

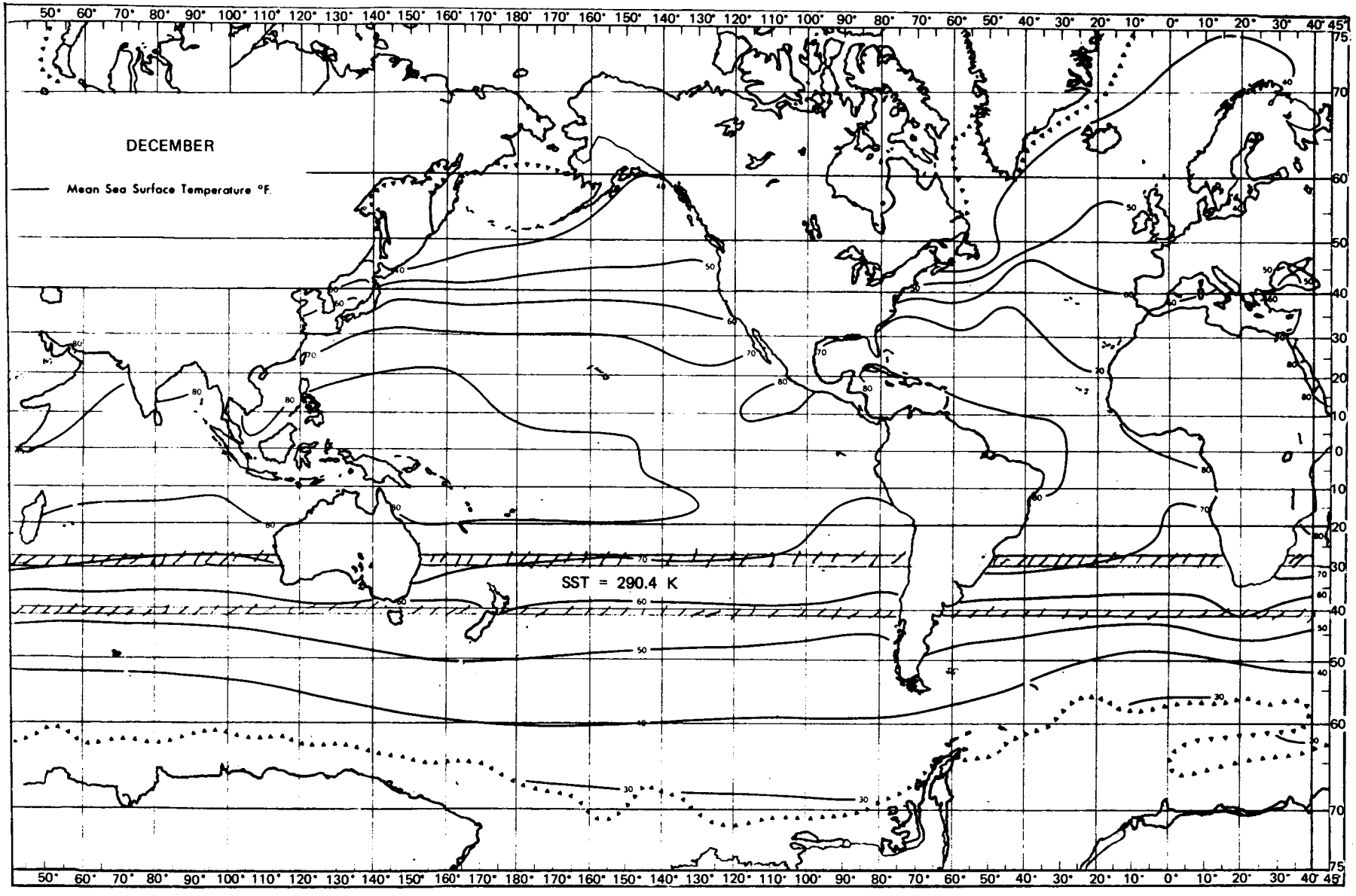

Figure 6.

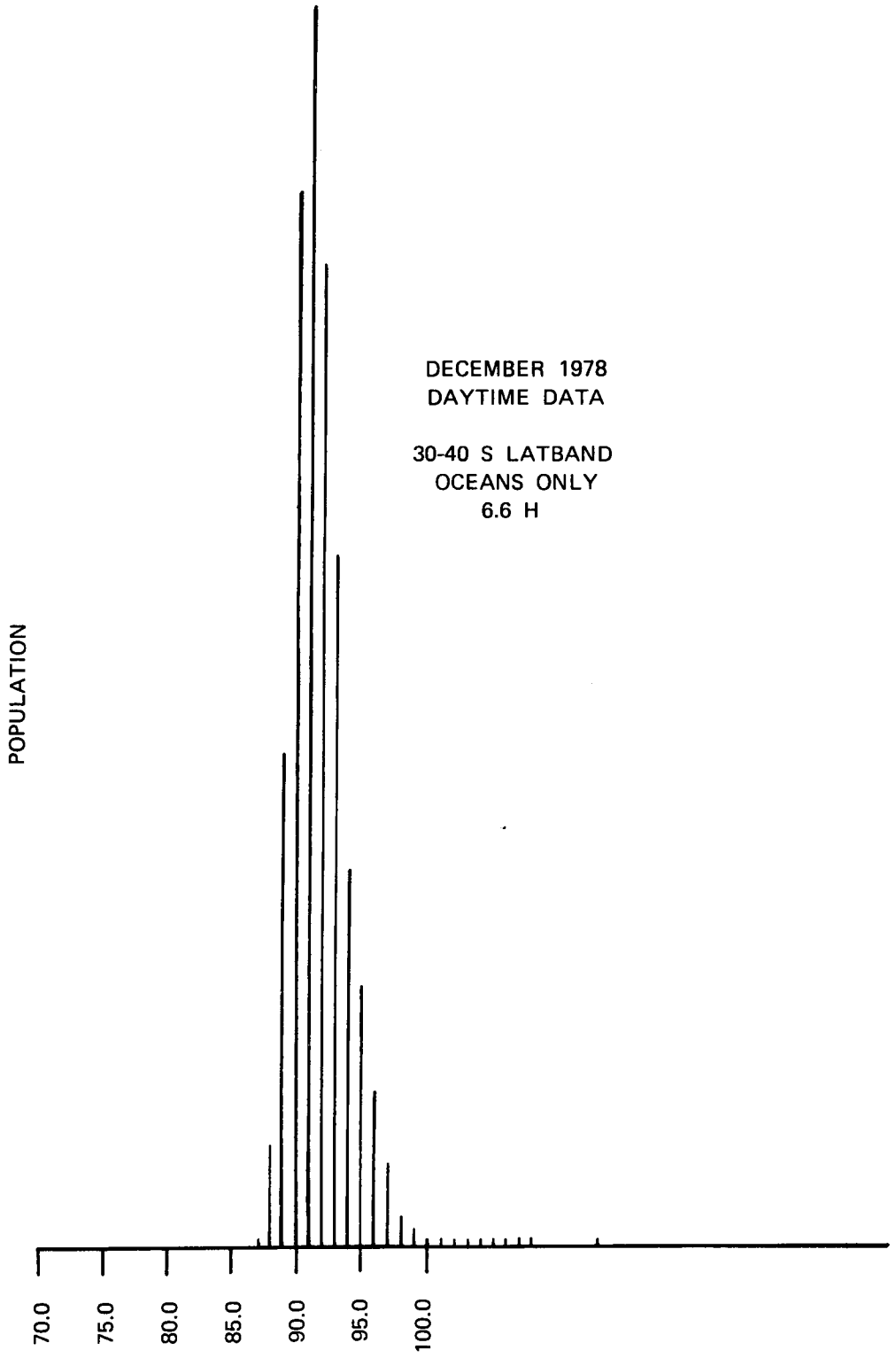
DECEMBER 1978
DAYTIME DATA
30-40 S LATBAND
OCEANS ONLY
6.6 H
POPULATION
70.0
75.0
80.0
85.0
90.0
95.0
100.0

Figure 7.

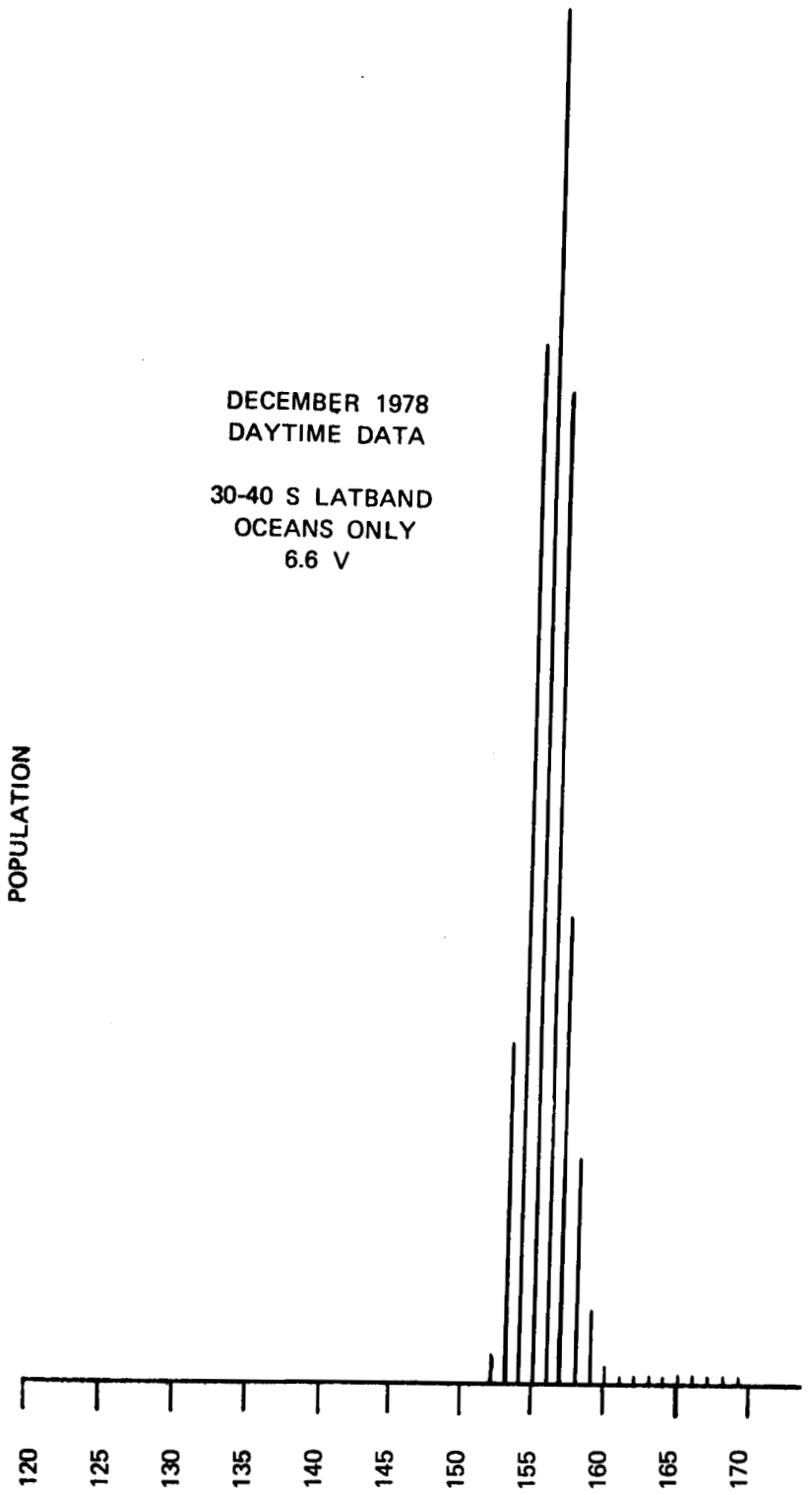
DECEMBER 1978
DAYTIME DATA
30-40 S LATBAND
OCEANS ONLY
6.6 V
POPULATION
120
125
130
135
140
145
150
155
160
165
170

Figure 8.

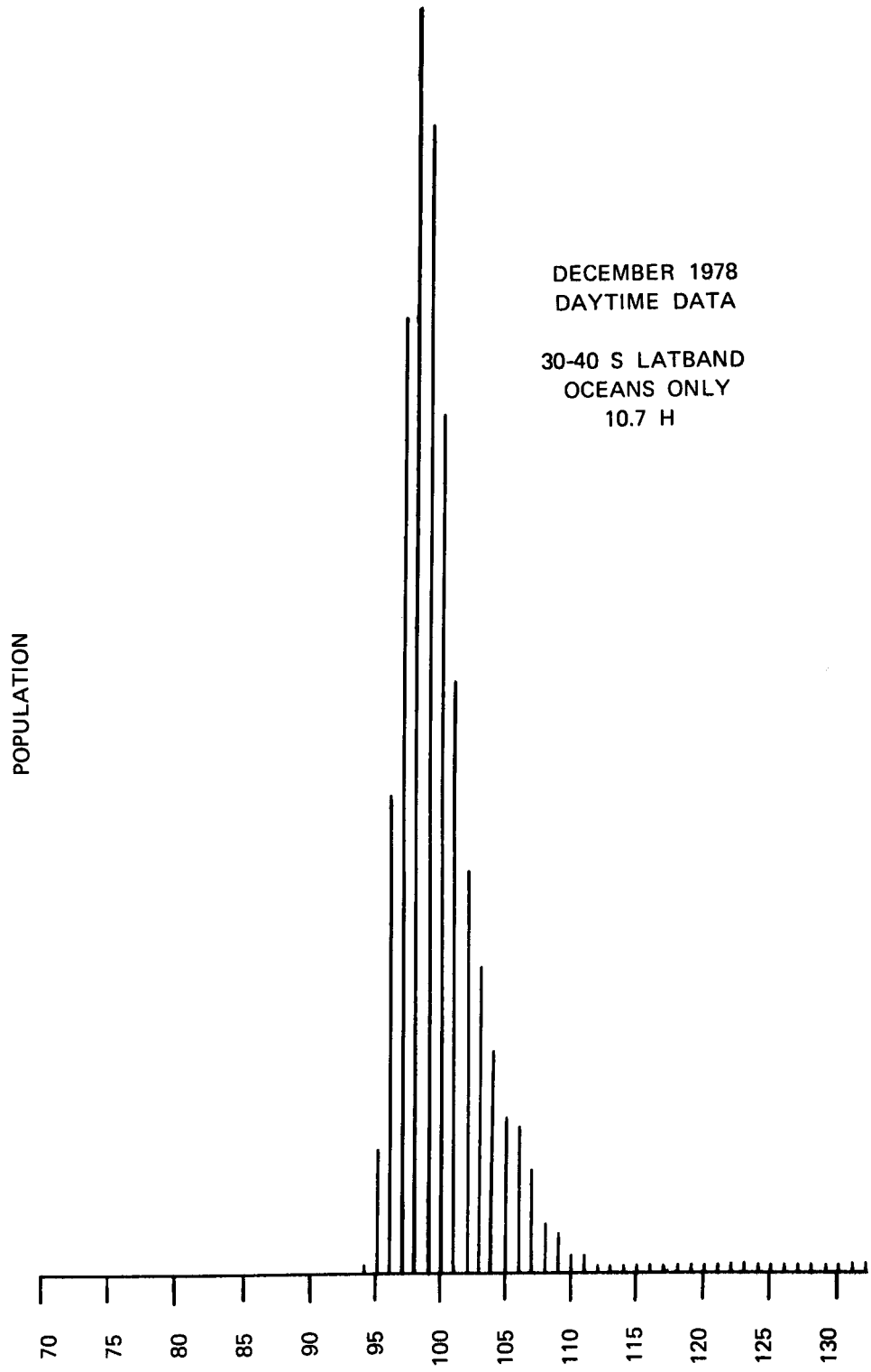
DECEMBER 1978
DAYTIME DATA
30-40 S LATBAND
OCEANS ONLY
10.7 H
POPULATION
70
75
80
85
90
95
100
105
110
115
120
125
130

Figure 9.

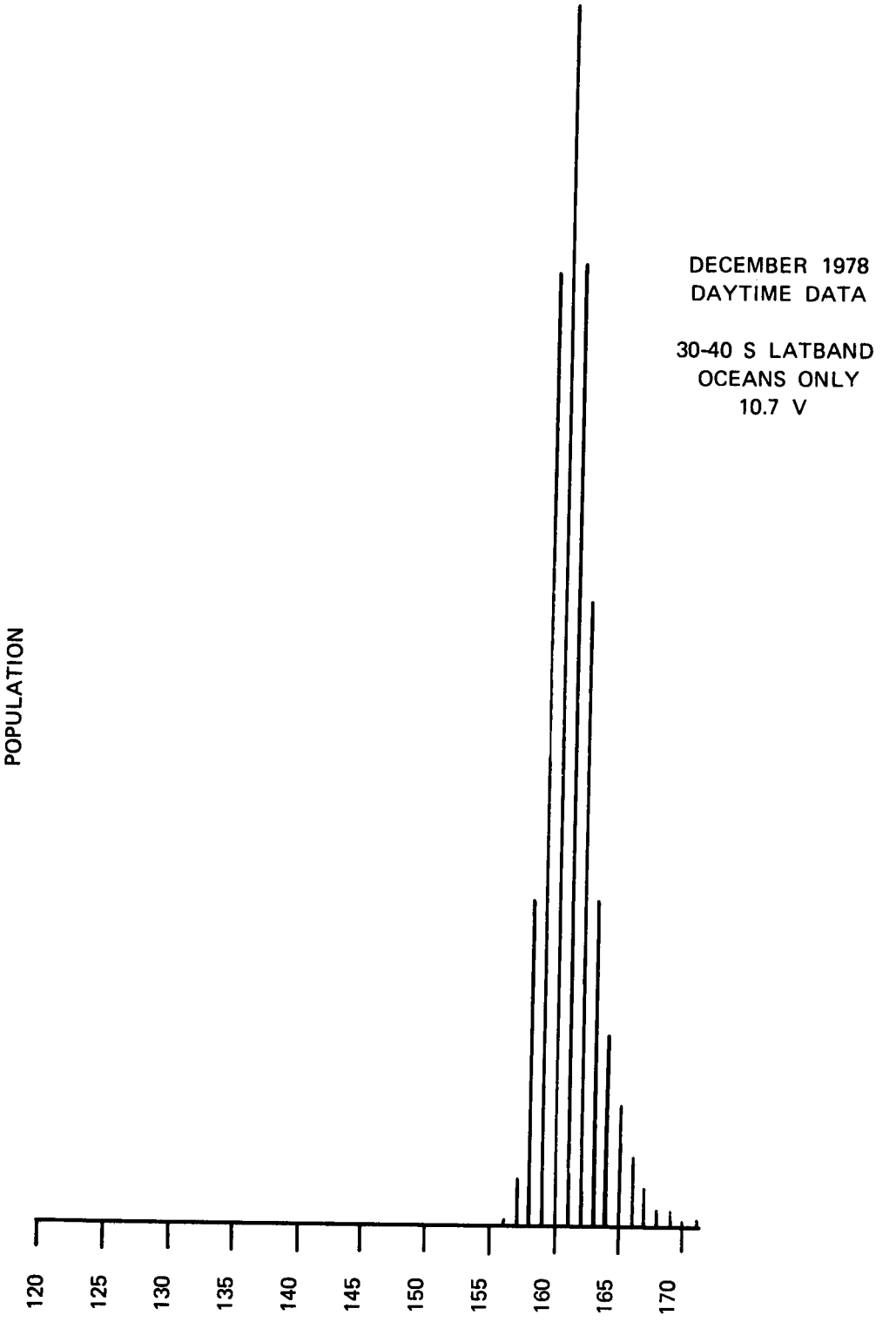
DECEMBER 1978
DAYTIME DATA
30-40 S LATBAND
OCEANS ONLY
10.7 V
POPULATION
120
125
130
135
140
145
150
155
160
165
170

Figure 10.

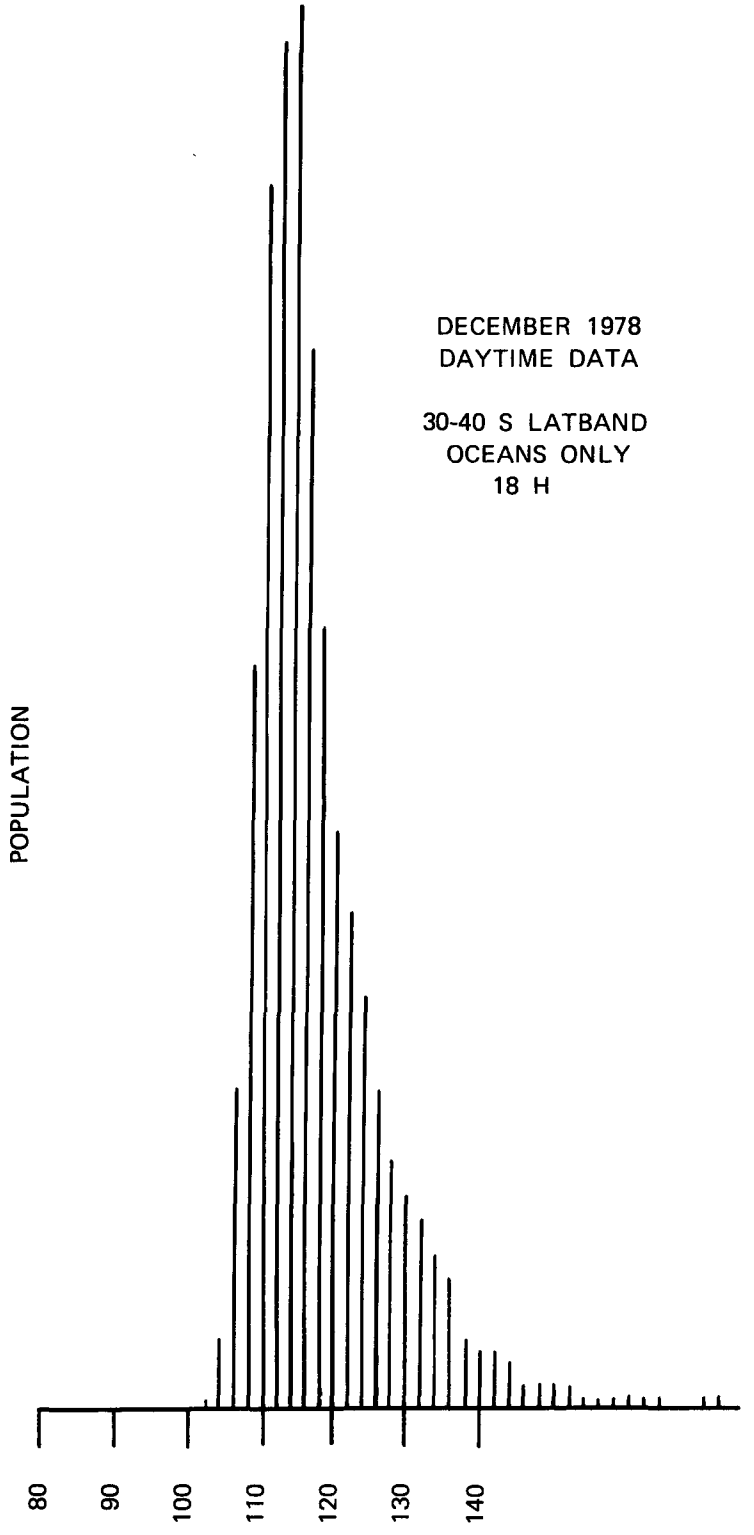
DECEMBER 1978
DAYTIME DATA
30-40 S LATBAND
OCEANS ONLY
18 H
POPULATION
80
90
100
110
120
130
140

Figure 11.

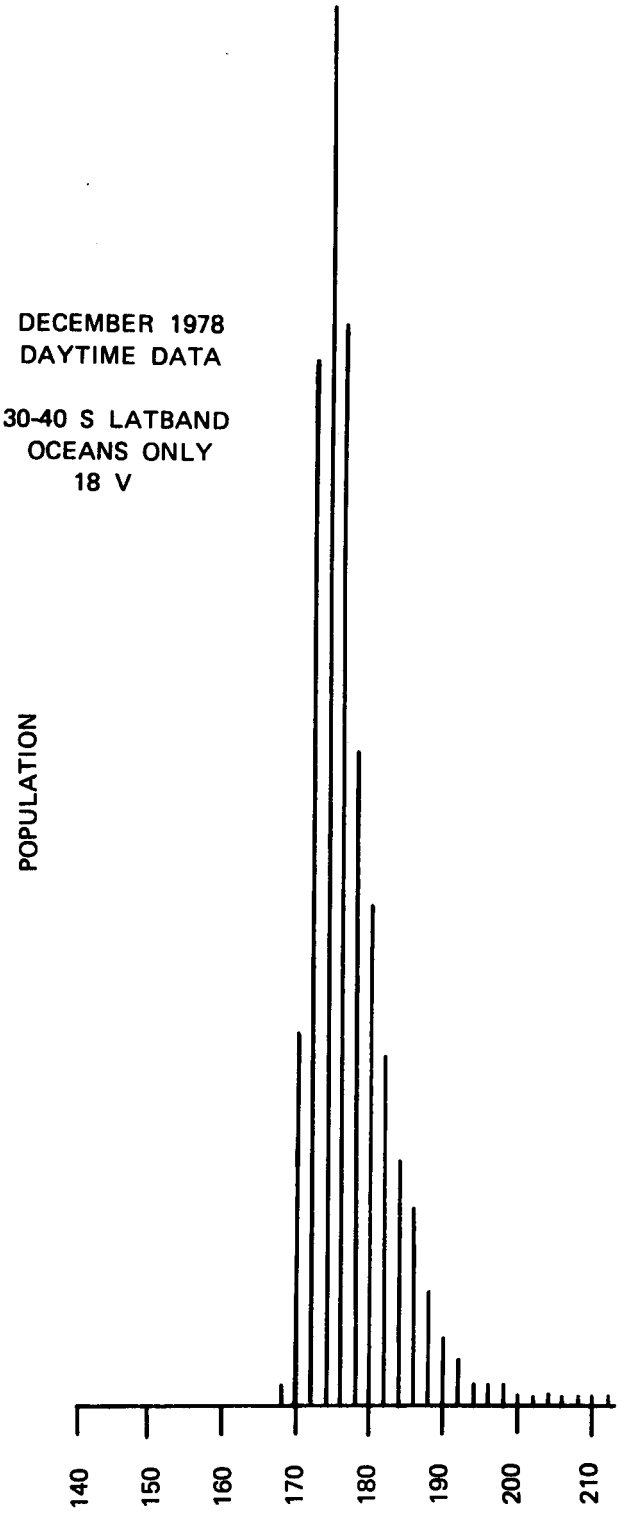
DECEMBER 1978
DAYTIME DATA
30-40 S LATBAND
OCEANS ONLY
18 V
POPULATION
140
150
160
170
180
190
200
210

Figure 12.

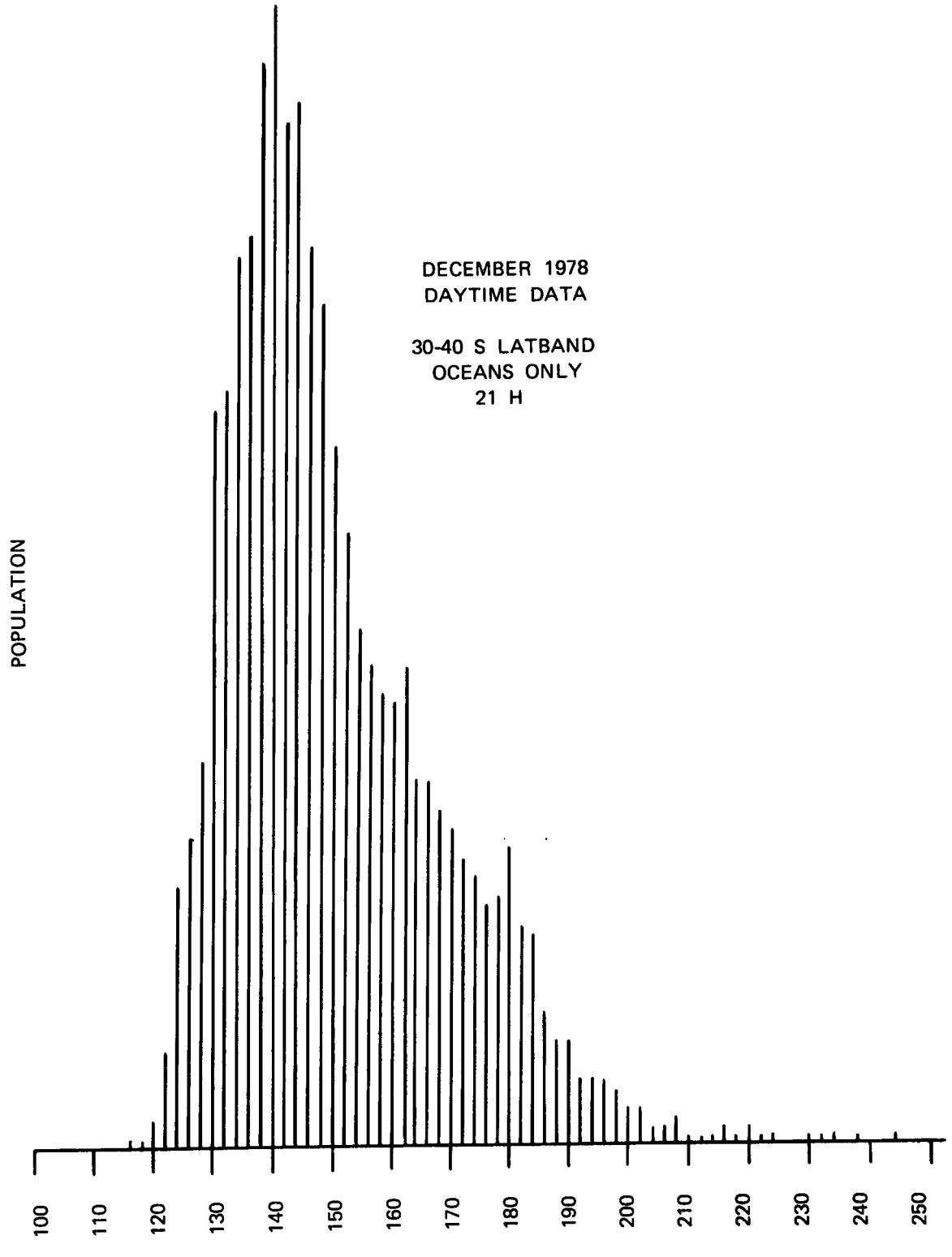
DECEMBER 1978
DAYTIME DATA
30-40 S LATBAND
OCEANS ONLY
21 H
POPULATION
100
110
120
130
140
150
160
170
180
190
200
210
220
230
240
250

Figure 13.

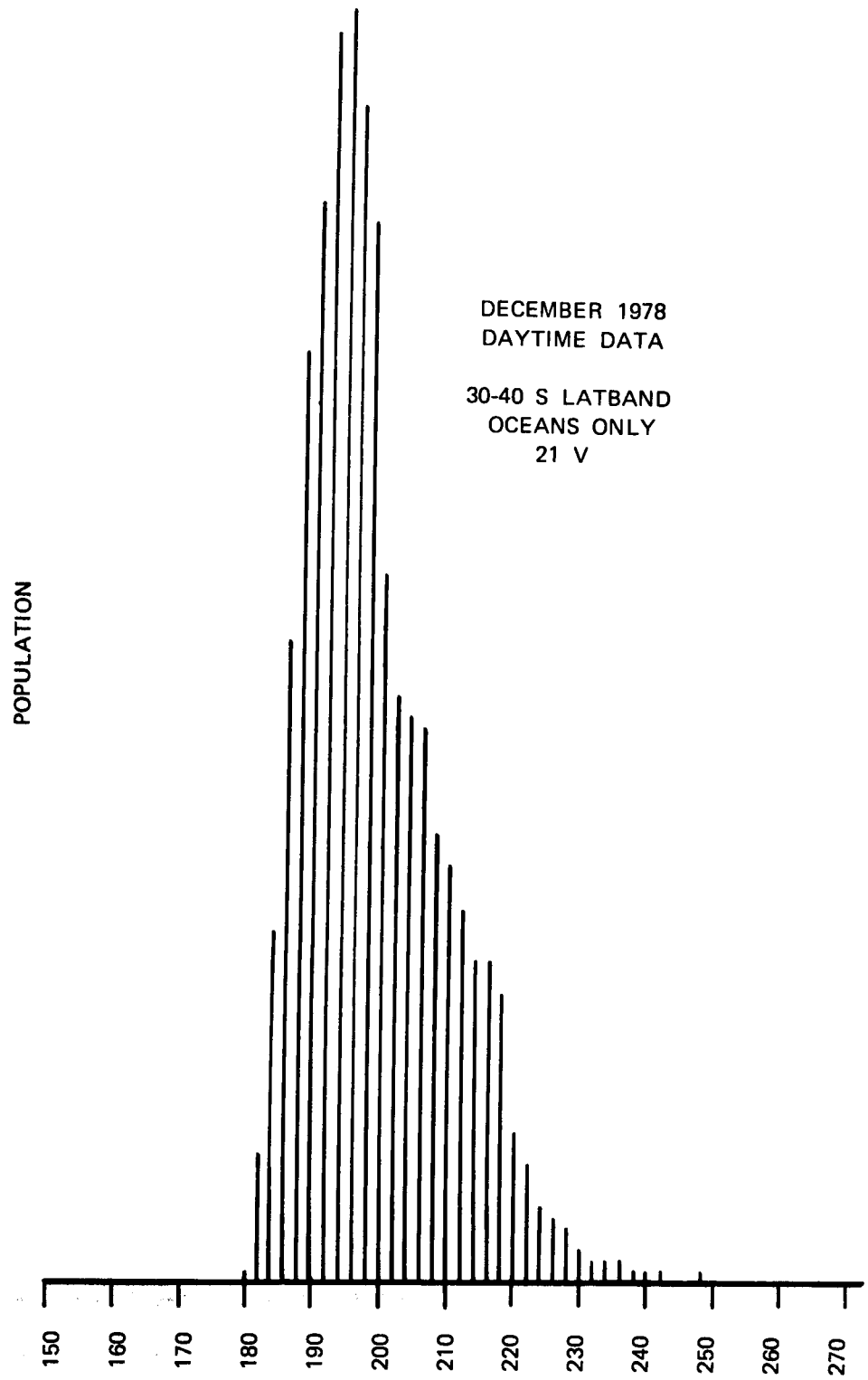
DECEMBER 1978
DAYTIME DATA
30-40 S LATBAND
OCEANS ONLY
21 V
POPULATION
150
160
170
180
190
200
210
220
230
240
250
260
270

Figure 14.

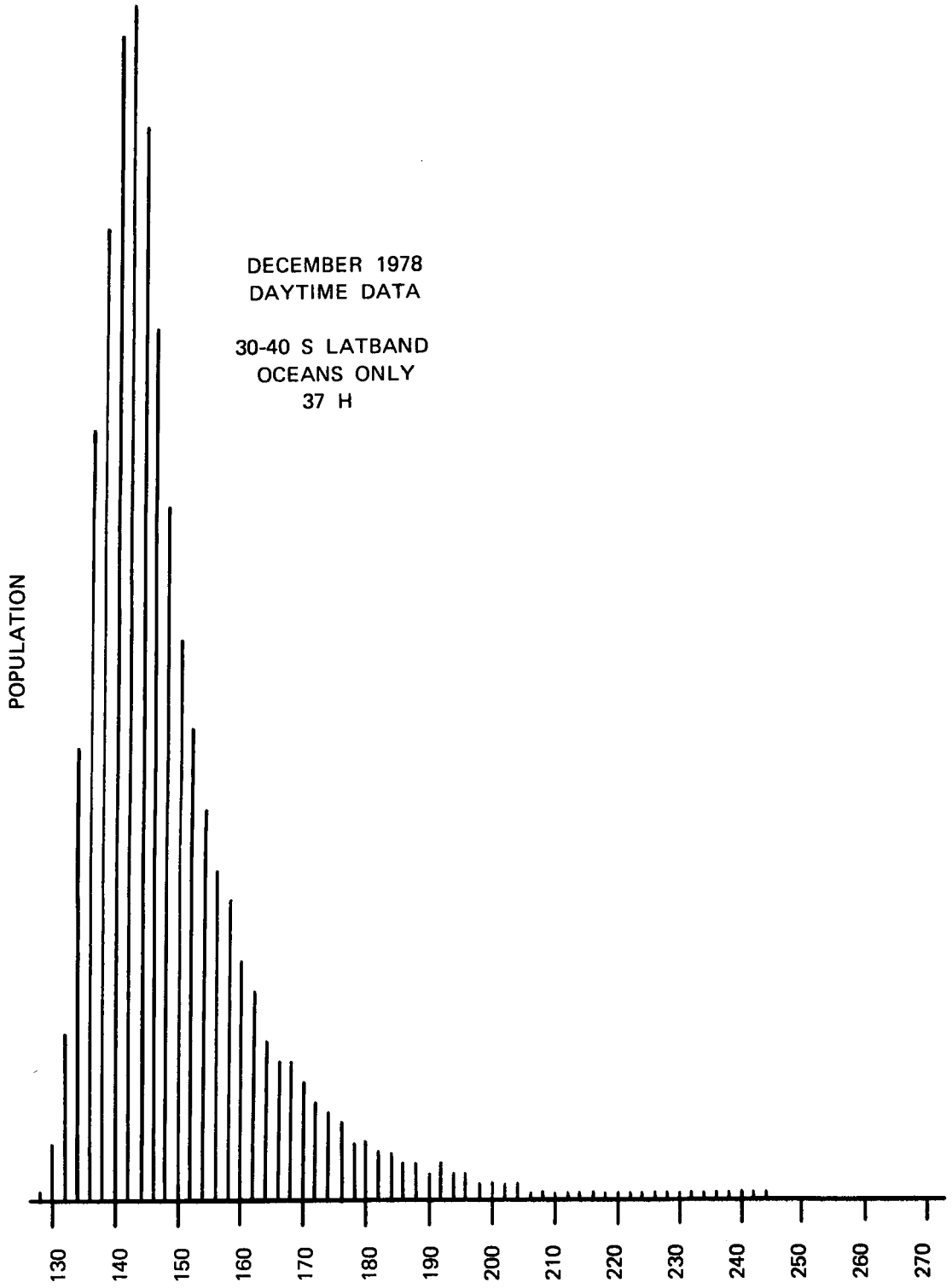
DECEMBER 1978
DAYTIME DATA
30-40 S LATBAND
OCEANS ONLY
37 H
POPULATION
130
140
150
160
170
180
190
200
210
220
230
240
250
260
270

Figure 15.

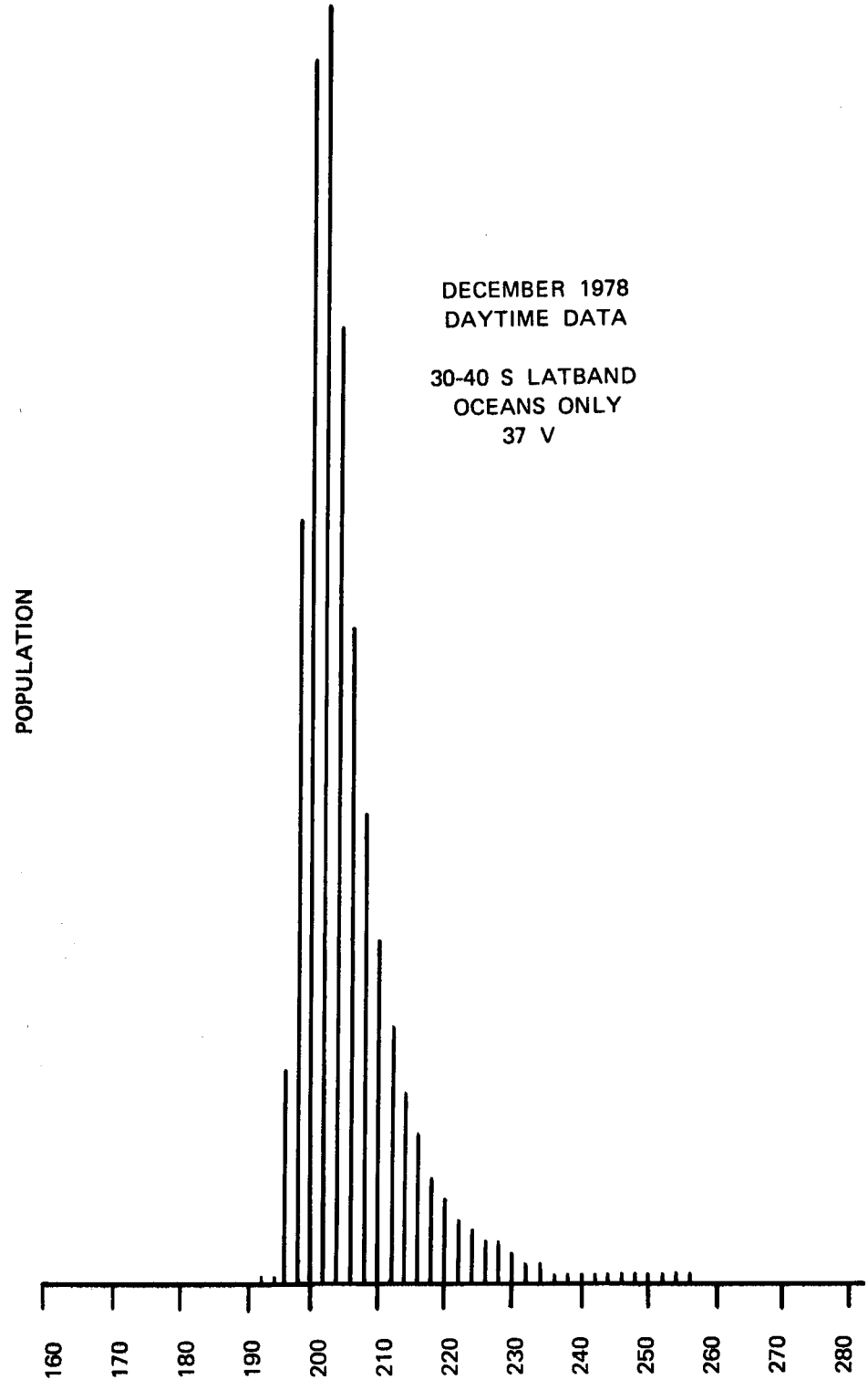
DECEMBER 1978
DAYTIME DATA
30-40 S LATBAND
OCEANS ONLY
37 V
POPULATION
160
170
180
190
200
210
220
230
240
250
260
270
280

Figure 16.

Table 4.

Wavelength (cm)	4.6	2.7	1.7	1.4	0.81
H-adjustments (K)	-5.9	-7.1	-4.2	-1.2	-1.7
V-adjustment (K)	2.2	2.3	2.9	2.5	4.6

Table 5.

Channel	a	b	a'	b'
4.6 H	-4.9	1.068	-2.6	1.005
V	15.5	1.017	18.0	0.939
2.7 H	-1.9	1.042	-1.4	1.001
V	15.5	0.990	16.3	0.950
1.7 H	-7.6	1.047	-5.8	1.017
V	22.4	0.948	24.9	0.913
1.4 H	-27.0	1.113	-27.5	1.091
V	14.8	0.974	25.4	0.902
0.81 H	-8.8	1.040	-2.1	0.989
V	27.9	0.920	28.0	0.905

These agree within 5 K for the horizontal polarization channels at the 0.8, 1.7, 2.8, and 4.6 cm wavelengths. However, the corresponding vertical polarization channels show discrepancies of about 10 K. The worst discrepancy is for the 1.4 H channel, about 16 K. On the other hand, the 1.4 V channel discrepancy is only about 8 K. In these figures, the two heavy clusters of points represent oceanic areas at the low radiance end and sea ice at the higher radiance end; land values are masked out. The width of the distribution, especially noticeable between the two clusters, is due to the different averaging of IFOVs containing mixtures of ocean with land and sea ice in the CELLs and TCTs. In Table 5, the primed and unprimed values of a and b differ because the former include a correction for the space spillover fraction and the CELLs already take into account the spillover into space.

In summary, the procedures outlined above (see also discussion of errors from the model calculations in Appendix A.) are estimated to give radiances to within 2 K for the 1.7, 2.7, and 4.6 cm channels and within 5 K for the 0.8 and 1.4 cm channels, at the time of the corrections. Presuming these estimates to be correct, they imply worse errors in the CELL tape radiances for some of the channels, as illustrated in Figures 17-26.

As a final note, the TCT polarization differences over open ocean in the north polar region have been found to be in good agreement (within 2 K) with radiometric measurements obtained during the NORSEX-79 mission (Maetzler, et al., 1984).

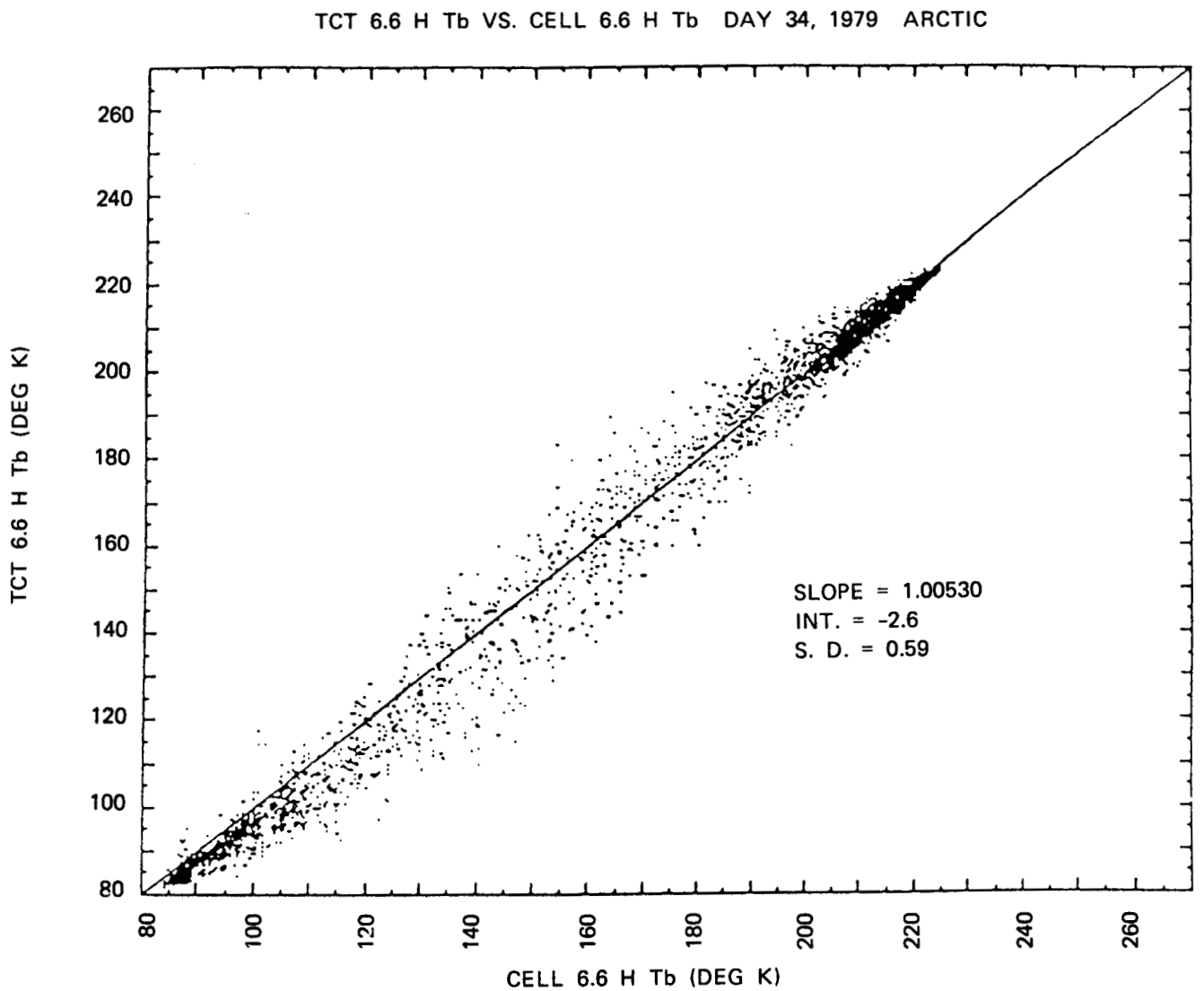
TCT 6.6 H Tb VS. CELL 6.6 H Tb DAY 34, 1979 ARCTIC
TCT 6.6 H Tb (DEG K)
CELL 6.6 H Tb (DEG K)
SLOPE = 1.00530
INT. = -2.6
S. D. = 0.59
80
100
120
140
160
180
200
220
240
260

Figure 17.

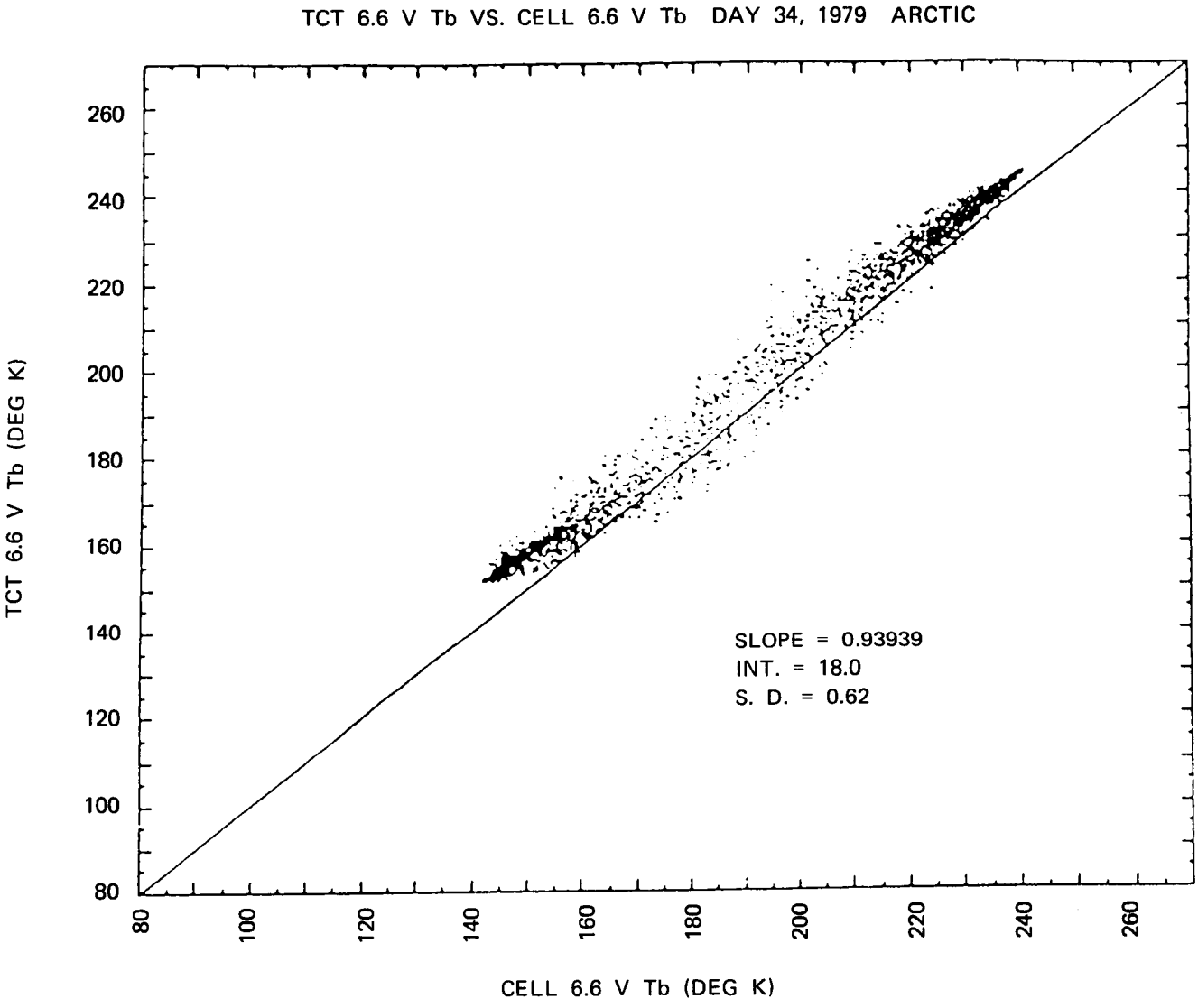
TCT 6.6 V Tb VS. CELL 6.6 V Tb DAY 34, 1979 ARCTIC
TCT 6.6 V Tb (DEG K)
CELL 6.6 V Tb (DEG K)
SLOPE = 0.93939
INT. = 18.0
S. D. = 0.62
80
100
120
140
160
180
200
220
240
260

Figure 18.

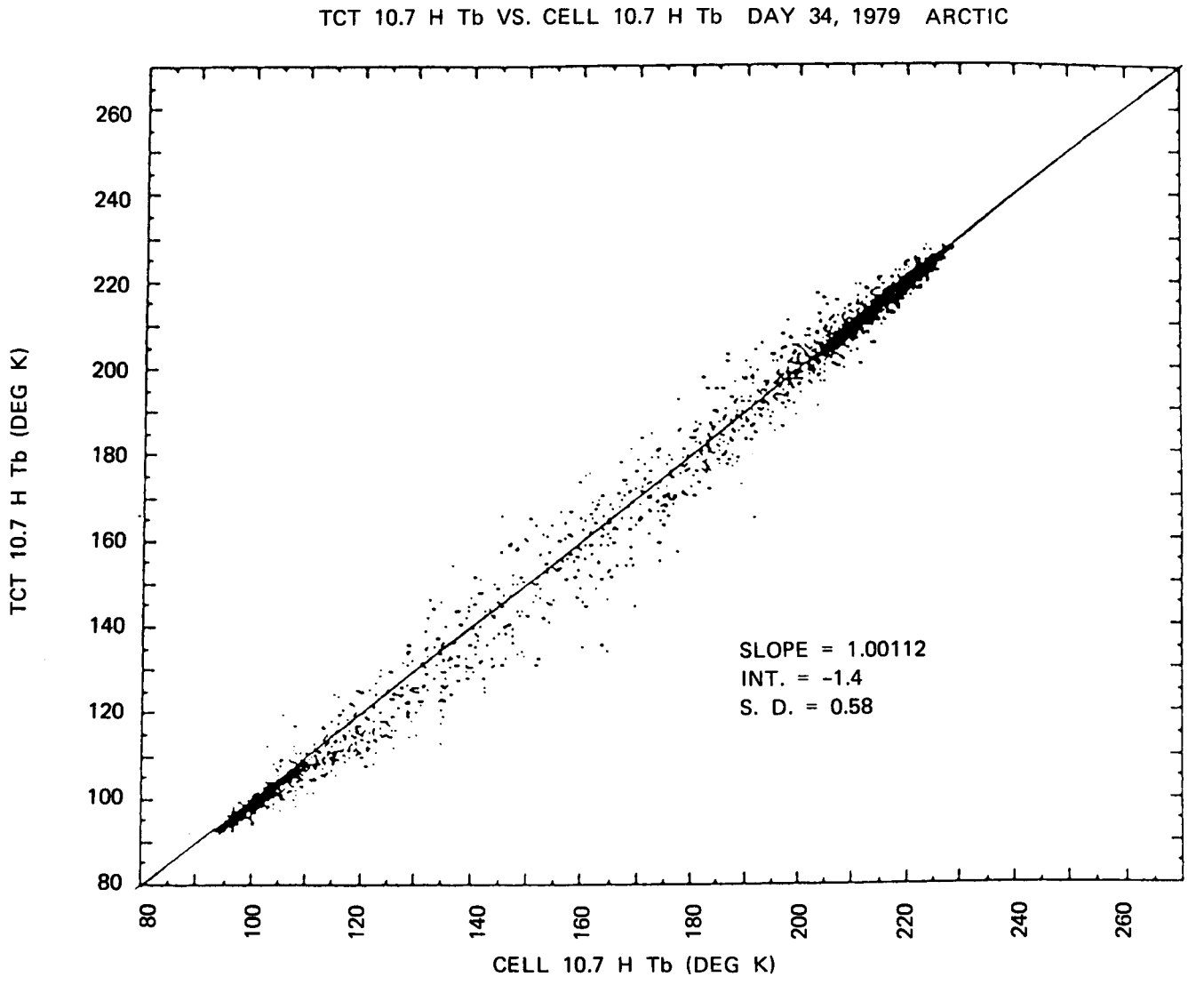
TCT 10.7 H Tb VS. CELL 10.7 H Tb DAY 34, 1979 ARCTIC
TCT 10.7 H Tb (DEG K)
CELL 10.7 H Tb (DEG K)
SLOPE = 1.00112
INT. = -1.4
S. D. = 0.58
80
100
120
140
160
180
200
220
240
260

Figure 19.

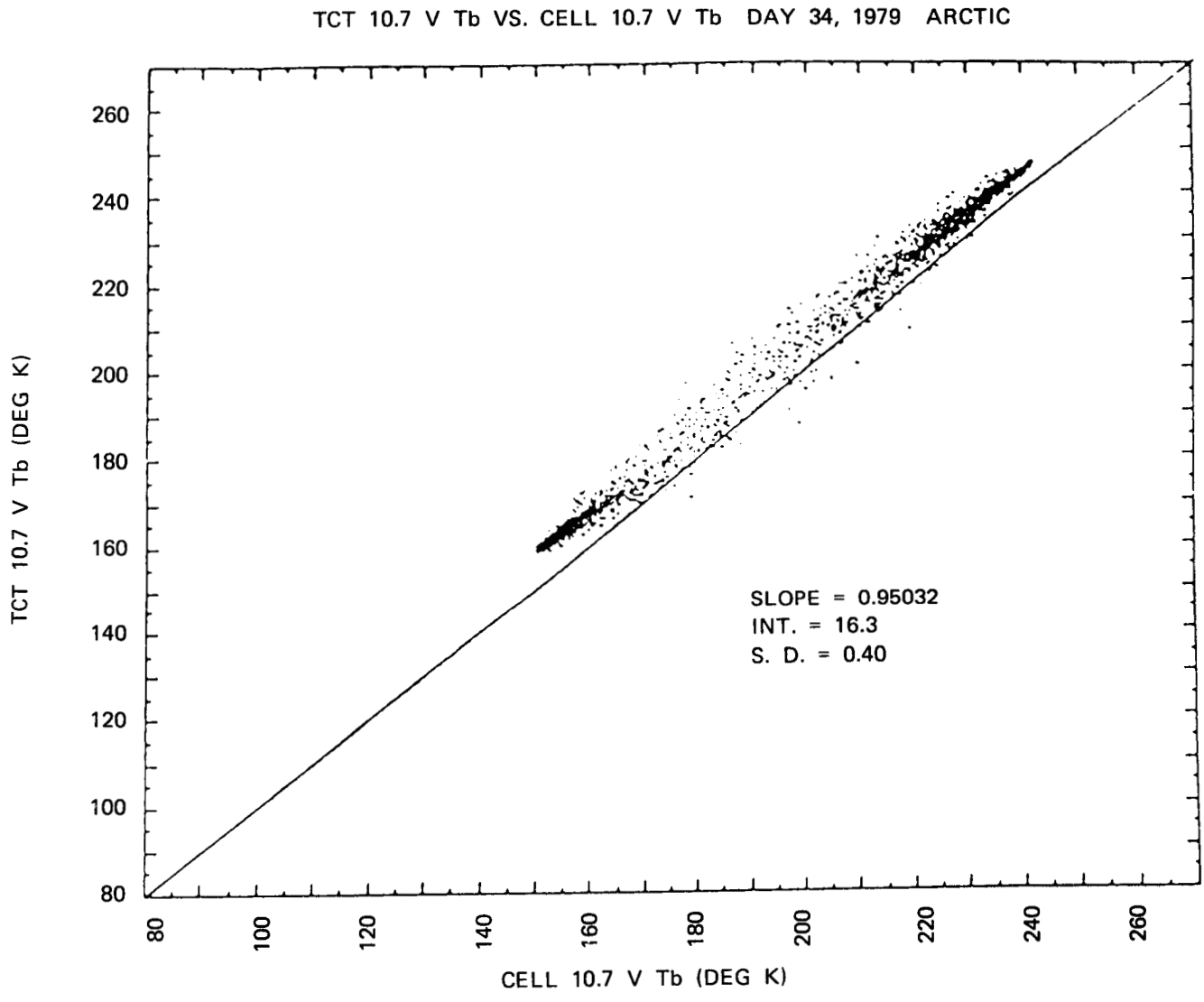
TCT 10.7 V Tb VS. CELL 10.7 V Tb DAY 34, 1979 ARCTIC
TCT 10.7 V Tb (DEG K)
CELL 10.7 V Tb (DEG K)
SLOPE = 0.95032
INT. = 16.3
S. D. = 0.40
80
100
120
140
160
180
200
220
240
260

Figure 20.

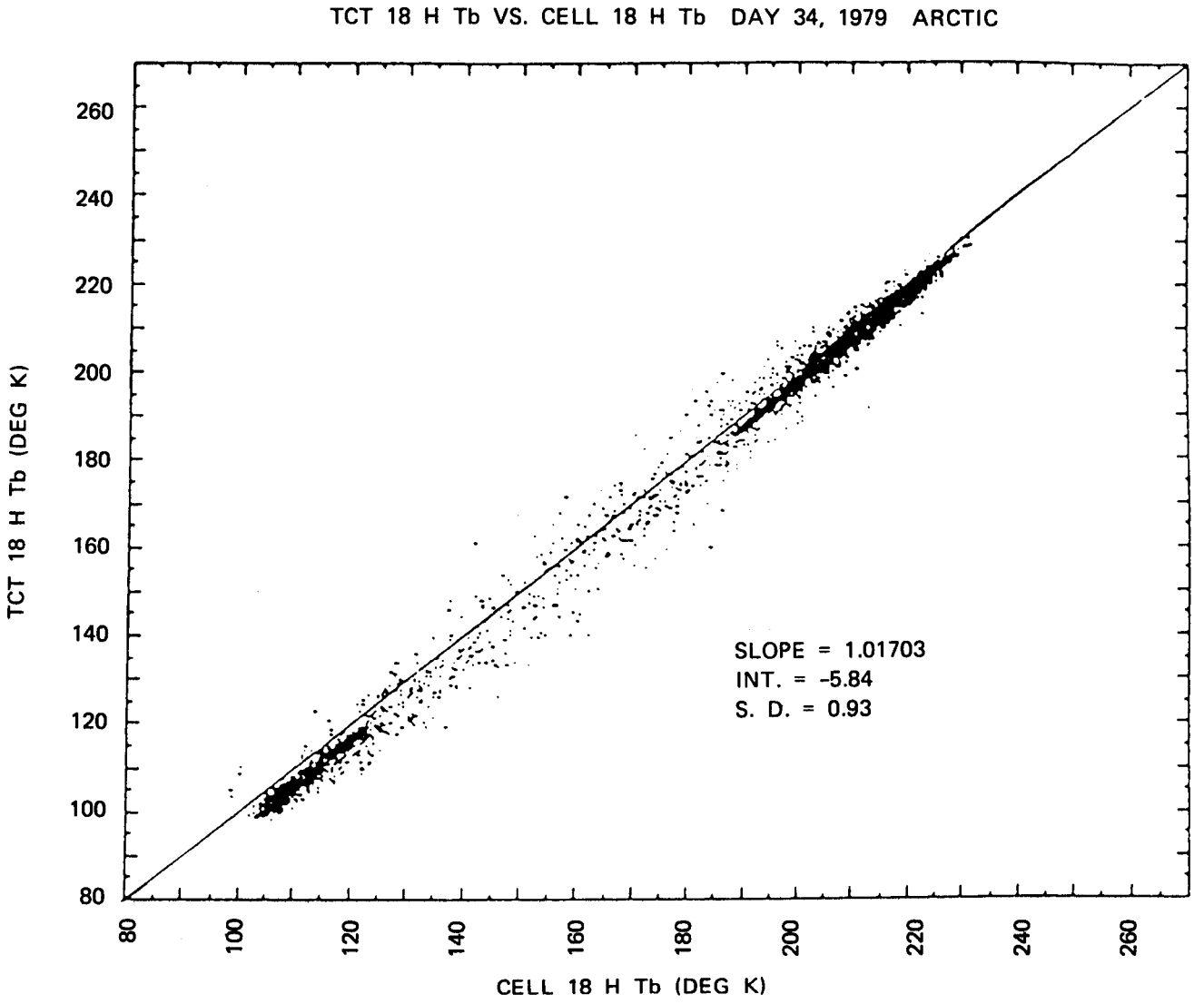
TCT 18 H Tb VS. CELL 18 H Tb DAY 34, 1979 ARCTIC
TCT 18 H Tb (DEG K)
CELL 18 H Tb (DEG K)
SLOPE = 1.01703
INT. = -5.84
S. D. = 0.93
80
100
120
140
160
180
200
220
240
260

Figure 21.

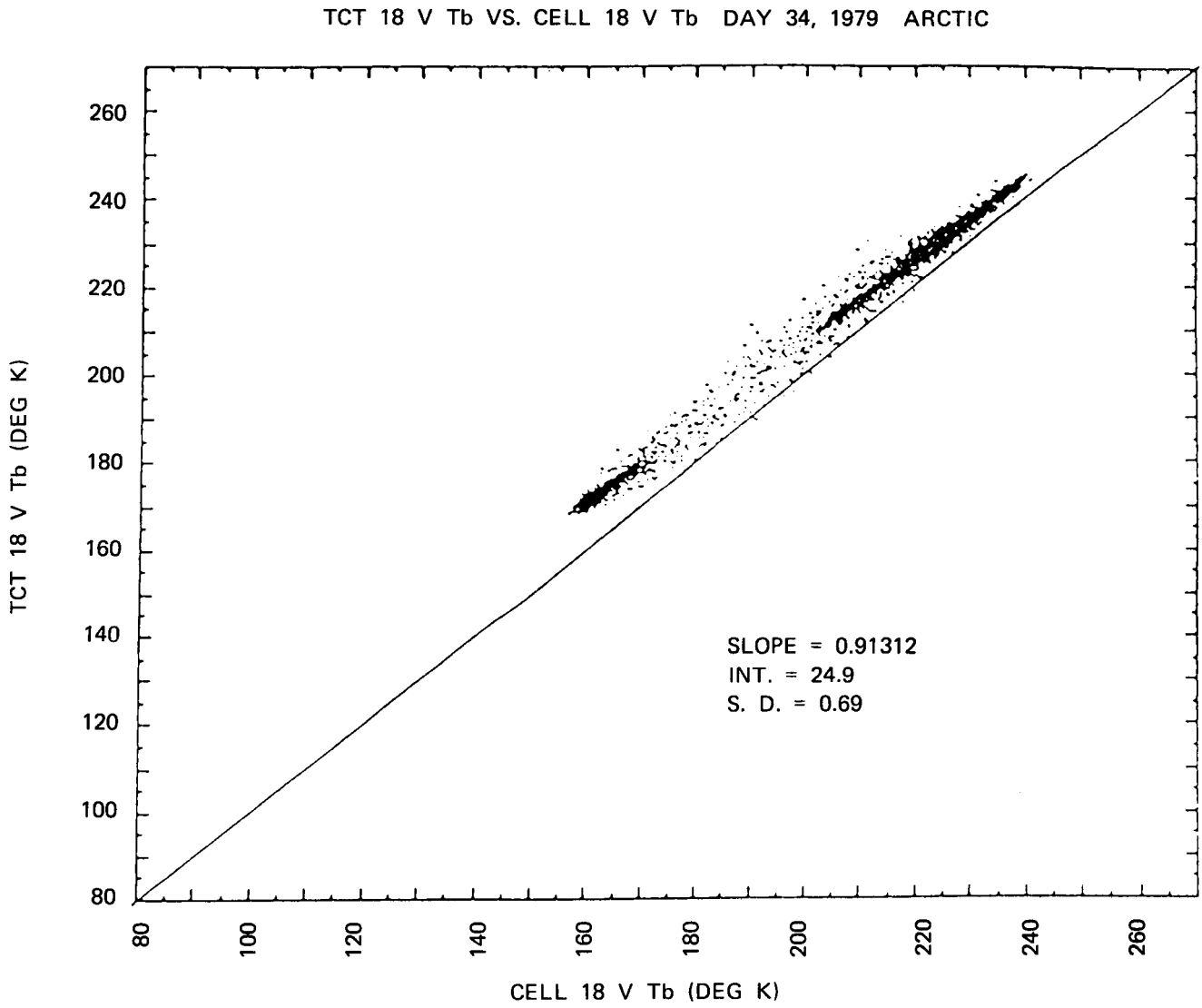
TCT 18 V Tb VS. CELL 18 V Tb DAY 34, 1979 ARCTIC
TCT 18 V Tb (DEG K)
CELL 18 V Tb (DEG K)
SLOPE = 0.91312
INT. = 24.9
S. D. = 0.69
80
100
120
140
160
180
200
220
240
260

Figure 22.

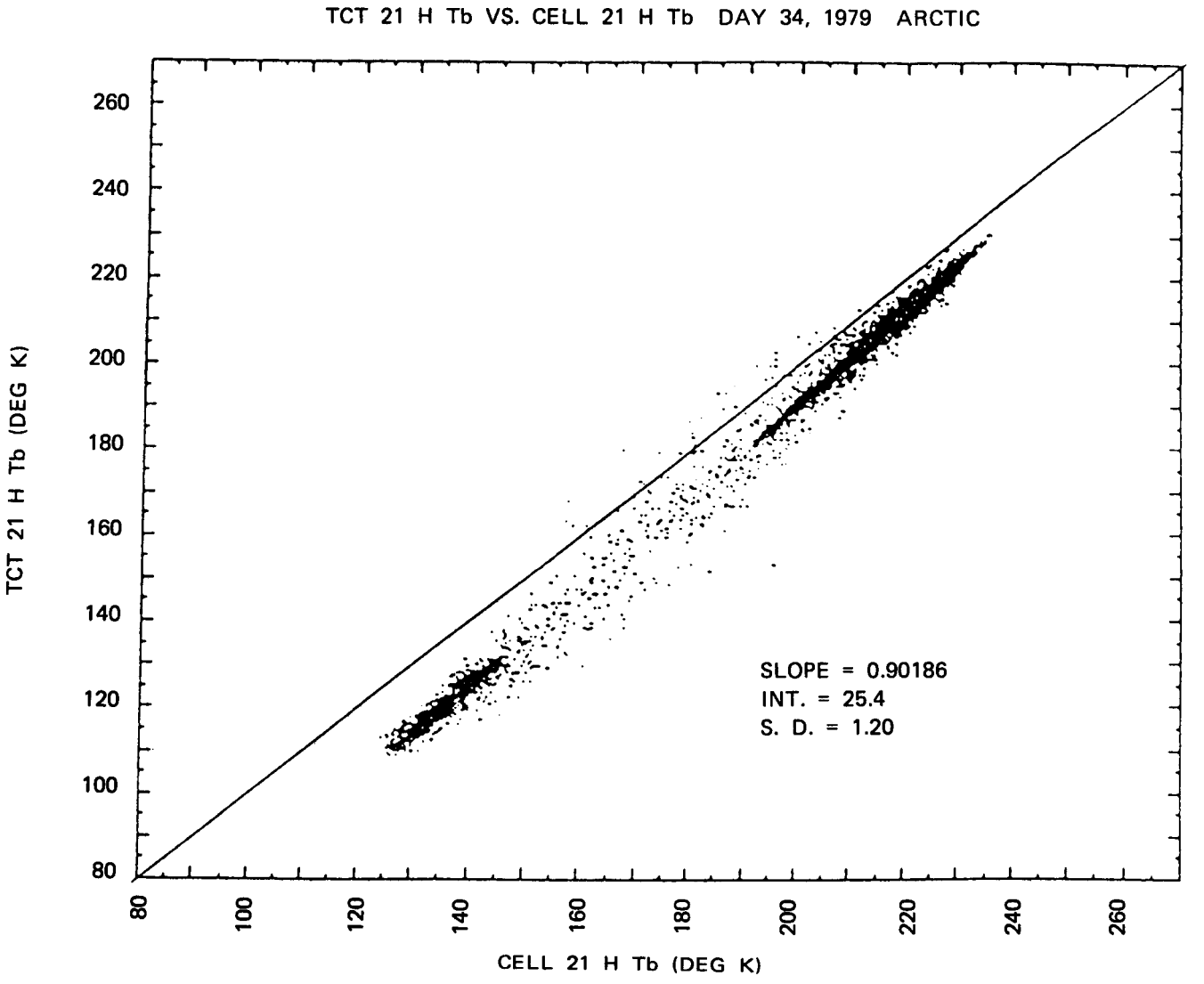
TCT 21 H Tb VS. CELL 21 H Tb DAY 34, 1979 ARCTIC
TCT 21 H Tb (DEG K)
CELL 21 H Tb (DEG K)
SLOPE = 0.90186
INT. = 25.4
S. D. = 1.20
80
100
120
140
160
180
200
220
240
260

Figure 23.

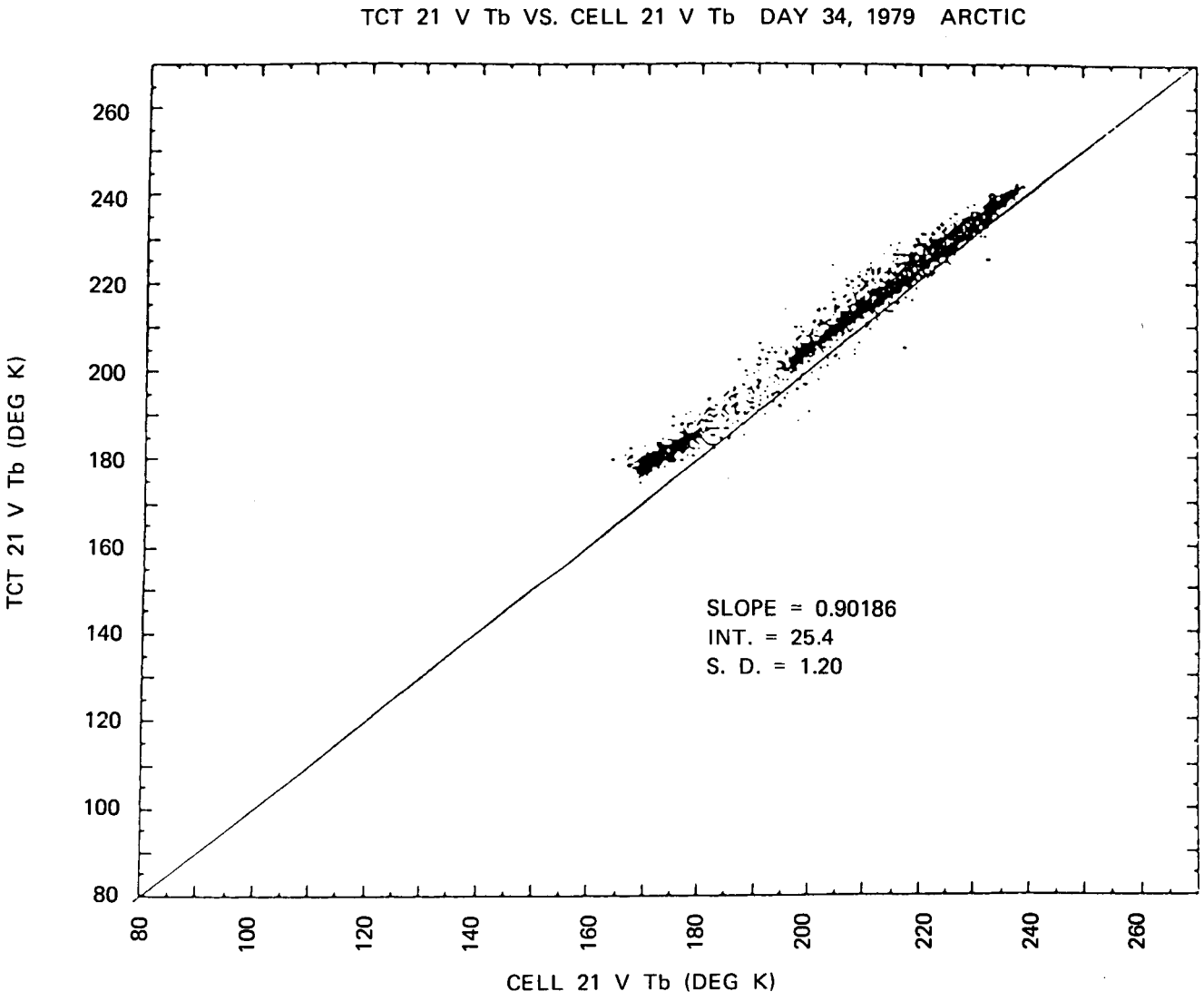
TCT 21 V Tb VS. CELL 21 V Tb DAY 34, 1979 ARCTIC
TCT 21 V Tb (DEG K)
CELL 21 V Tb (DEG K)
SLOPE = 0.90186
INT. = 25.4
S. D. = 1.20
80
100
120
140
160
180
200
220
240
260

Figure 24.

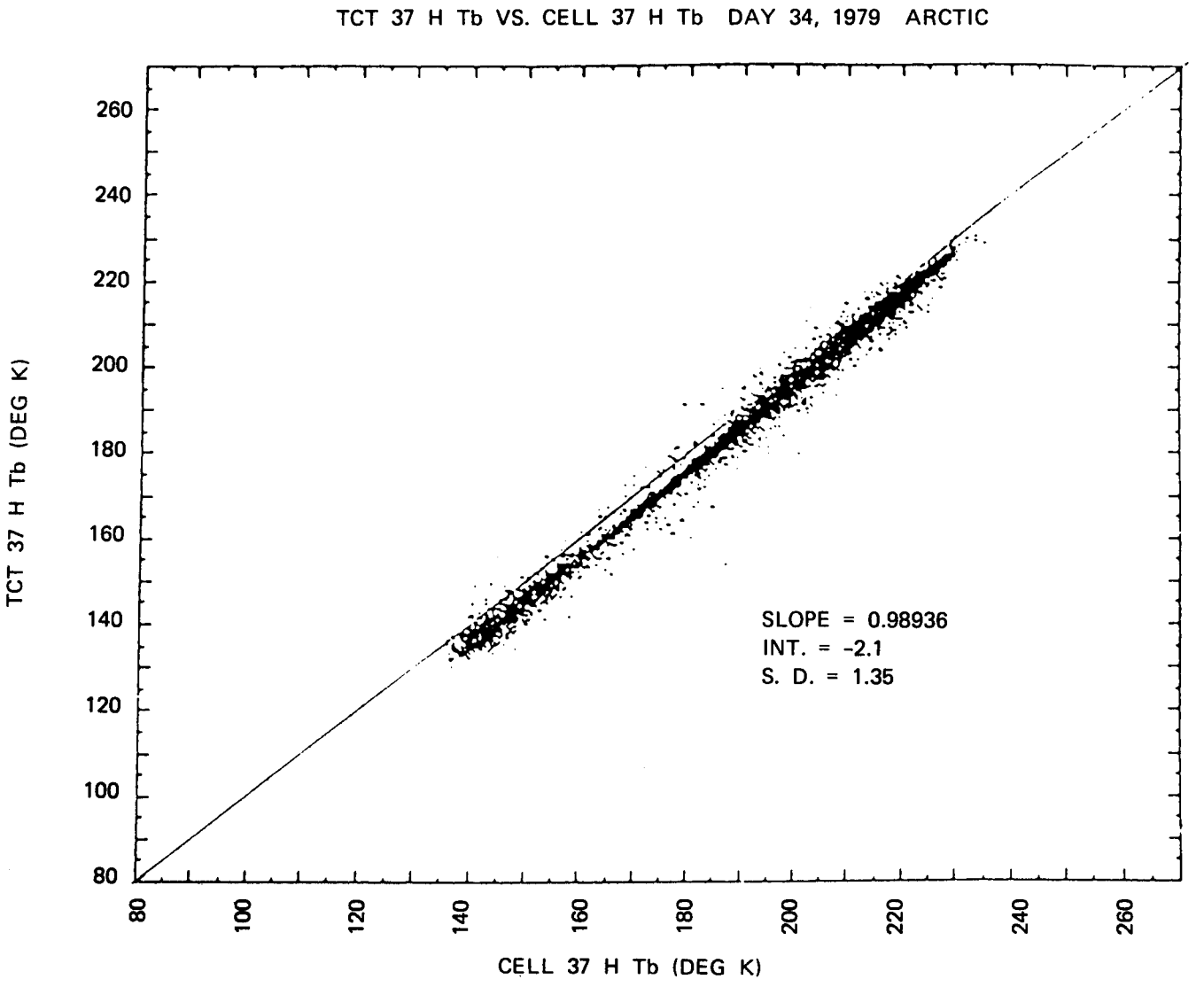
TCT 37 H Tb VS. CELL 37 H Tb DAY 34, 1979 ARCTIC
TCT 37 H Tb (DEG K)
CELL 37 H Tb (DEG K)
SLOPE = 0.98936
INT. = -2.1
S. D. = 1.35
80
100
120
140
160
180
200
220
240
260

Figure 25.

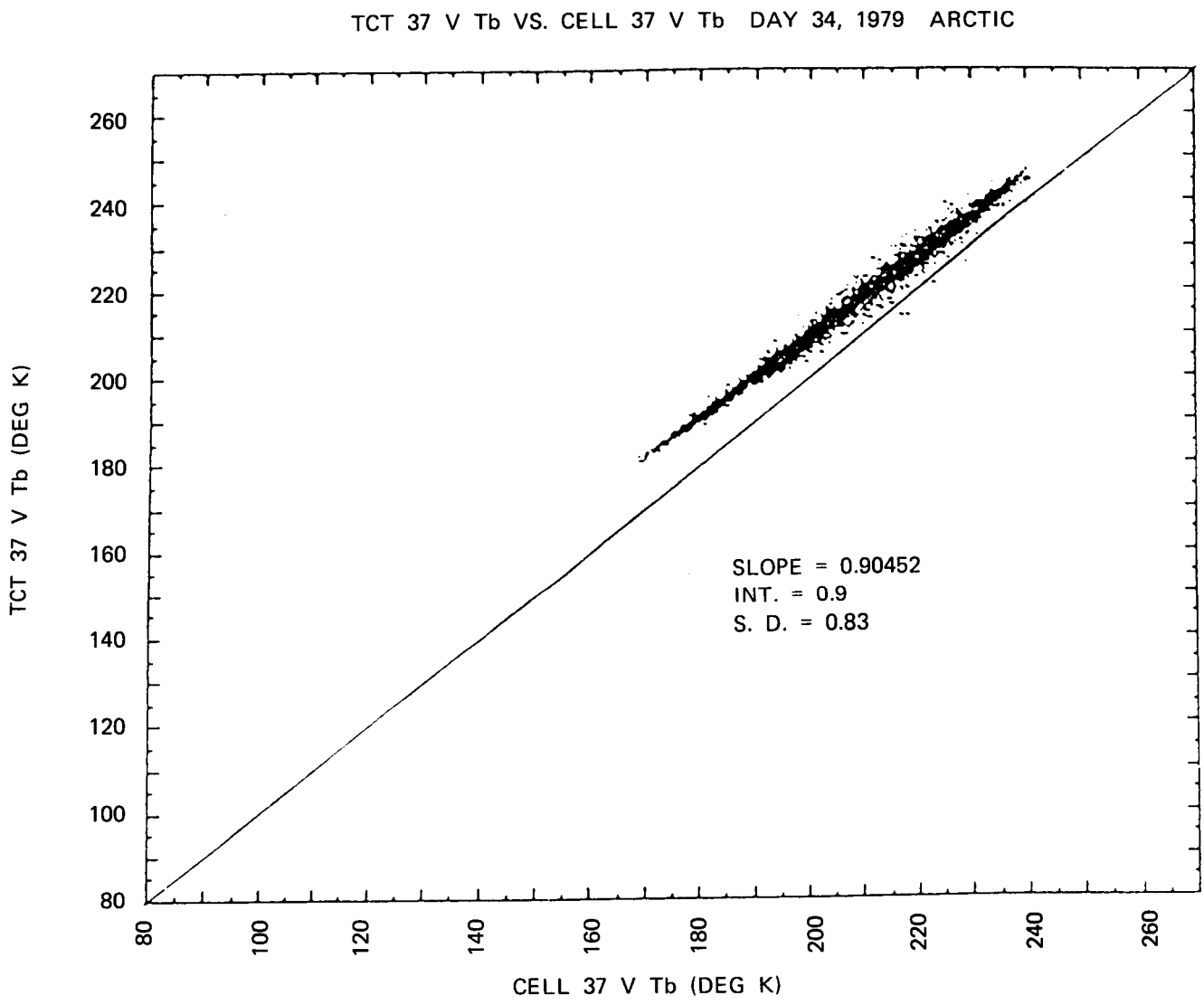
TCT 37 V Tb VS. CELL 37 V Tb DAY 34, 1979 ARCTIC
TCT 37 V Tb (DEG K)
CELL 37 V Tb (DEG K)
SLOPE = 0.90452
INT. = 0.9
S. D. = 0.83
80
100
120
140
160
180
200
220
240
260

Figure 26.

REFERENCES

Gloersen, P. and F. T. Barath, 1977, "A Scanning Multichannel Microwave Radiometer for the Nimbus-G and Seasat-A", *IEEE J. of Ocean Eng.* OE-2, pp. 172-178.

Gloersen, P., D. J. Cavalieri, and H. V. Soule, *An Alternative Algorithm for Correction of the Scanning Multichannel Microwave Radiometer Polarization Radiances Using Nimbus-7 Observed Data,* NASA TM-80672.

Gloersen, P., D. J. Cavalieri, A. T. C. Chang, T. T. Wilheit, W. J. Campbell, O. M. Johannessen, K. B. Katsoros, K. F. Kunzi, D. B. Ross, D. Staelin, E. P. L. Windsor, F. T. Barath, P. Gudmandsen, E. Langham, and R. O. Ramseier, 1984, "A Summary of Results from the First Nimbus-7 Observations", *J. Geophys. Res.,* 89, 5335-5344.

Gloersen, P., 1983, *Calibration of the Nimbus-7 SMMR: II Polarization Mixing Corrections,* NASA TM-84976.

Lane, J. A. and J. A. Saxton, 1952, "Dielectric Dispersion in Pure Polar Liquids at Very High Radio Frequencies", *Roy. Soc. London* A213, pp. 400-408.

Gaut, N. E., 1968, "Studies of Atmospheric Water Vapor by Means of Passive Microwave Techniques", *M.I.T. Res. Lab. Electronics,* Tech. Report 467.

Gaut, N. E. and E. C. Reifenstein, III, 1970, "Interaction of Microwave Energy With the Atmosphere", *AIAA Earth Resources Observations and Informations Systems Conference, No. 70-197,* Annapolis, MD.

Maetzler, C., R. O. Ramseier, and E. Svendsen, 1984, "Polarization Effects in Sea-Ice Signatures", *IEEE J. Ocean Eng.* OE-9, pp. 333-338.

Njoku, E. G., J. M. Stacey, and F. T. Barath, 1980, "The Seasat Scanning Multichannel Microwave Radiometer (SMMR): Instrument Description and Performance", *IEEE J. Ocean Eng.* OE-5, pp. 100-115.

APPENDIX A – THE OCEAN/ ATMOSPHERE RADIATIVE TRANSFER MODEL

The model used in calculating the theoretical values of oceanic radiances in orbit is based on (1) the Kirchoff reflection coefficients of the calm ocean surface as obtained with the microwave dielectric coefficients for water as measured by Lane and Saxton (1952), (2) semi-empirical values for the absorptivity of oxygen, water vapor, and cloud droplets (Gaut, 1968; Gaut and Reifenstein, 1970), and (3) an empirical wind effect model based on limited comparisons of SMMR radiances and polarizations with near-surface winds obtained from NOAA buoys. The full-blown model (with different wind coefficients) is installed on the Goddard IBM 3081, complete with lapse-rate models for calculating the atmospheric contributions (Chang and Wilheit, priv. comm.). The model was parameterized (see Appendix B) for use on a desk-top computer with the aid of some select calculations made on the IBM 3081. The essence of the parameterized model is given here. The radiative transfer equation used has four terms,

$$TB = B1 + B2 + B3 + B4 \qquad (12)$$

where surface contribution is:

$$B1 = E1(N)*TS*EXP(-TU)$$

and E1(N) is the surface emissivity for each SMMR channel, TS is the physical temperature of the ocean surface, and TU is the atmospheric opacity. The upwelling atmospheric component is:

$$B2 = (1 - EXP(-TU))*TA$$

and TA is a weighted average of the atmospheric temperature profile (used in place of the atmospheric layers on the full-blown model). A similar approximation is used for the downwelling atmospheric contribution, which is given by:

$$B3 = (1 - E1(N))*(1 - EXP(-TU)*TA*EXP(-TU)$$

The contribution from free space is:

$$B4 = (1 - E1(N))*2.7*EXP(-2*TU)$$

The surface emissivity is dependent on both the surface temperature, TS, and the near-surface winds, NSW, as follows:

$$E1(N) = A0(N) + A1(N)*(TS-271) + A2(N)*$$

$$(TS2-2712) + (B(N)/291)*NSW + (A(N)/291)*NSW2$$

The temperature coefficients. Ai(N), and the wind speed coefficients, A(N) and B(N), are given in the data statements of the model program listing in Appendix A. The temperature coefficients were obtained from Lane and Saxton (1952) and the wind coefficients A(N) and B(N) represent slopes of the curves of radiance, TB, vs observed wind speeds from the NOAA buoys. The latter are divided by 291, an average SST estimated for the buoy environment, so as to obtain an emissivity correction. Also, in calculating the V polarization emissivity correction, the wind speeds, WS, are limited to values greater than 7 m/s, since there is no experimental evidence to suggest emissivity changes at lower wind speeds in these channels.

The atmospheric opacity, TU, is composed of three factors, that due to water vapor, TV, that due to cloud droplets, TL, and that due to oxygen, OX, i.e.

$$TU = TV + TL + OX$$

where TV = 1.05E-03*W + 0.04E-03 for the 4.6 H & channels
= 3.10E-03*W + 0.10E-03 for the 2.7 H & V channels
= 1.94E-02*W + 0.30E-03 for the 1.7 H & V channels
= 6.78E-02*W + 0.50E-03 for the 1.4 H & V channels
= 3.29E-02*W + 1.20E-03 for the 0.8 H & V channels

and W is the input value of water vapor in cm in the column. The contribution from clouds is

$$TL = 2.61*L/(LAMBDA(N)^2)$$

where L is the input cloud droplet amount (in cm) in the column and LAMBDA(N) are the five SMMR wavelengths. Finally, the oxygen contribution is given by

$$OX = K(N)/TA$$

where K(N) is 3.8, 3.9, 4.5, 4.8, and 13.4 corresponding, respectively, to the SMMR wavelengths, 4.6, 2.7, 1.7, 1.4, and 0.81 cm, and TA is the input estimated weighted average of the atmospheric temperature profile.

An estimate of the errors in this approach can be made by examining the various terms in Equation (12) with regards to the values assumed for the parameters and the validity of the model. The estimate of the sea surface temperature was made using the December values of SST obtained from the U.S. Navy climatology for the 30-40°S latitude band (see Figure 21), and is probably the smallest source of error. The total variation in this zone is less than +/−3°C and the average is therefore probably accurate to less than +/−1°C, translating into radiance er-

rors of less than +/−0.5 K in the vertical channels and +/− 0.3 K in the horizontal channels. The climatological mean near-surface wind in this zone is 7 m/s, at which value the NSW contribution to the vertical radiances is negligible. Thus, if the NSW had been overestimated by 1 m/s, there would be no effect on the vertical channels and about a 1.5 K error on the horizontal channels. Underestimation by the same amount would lead to 0.5 K error in the vertical and 1.5 K error in the vertical and horizontal channels, respectively. By far the largest potential sources of error, especially at the shorter wavelengths, are the uncertainty of the selected values of cloudiness and water vapor used for calculating the atmospheric opacity. Errors arising from a 0.2 cm error in the estimation of water vapor in the column would be about 0.1, 0.5, 2, 7, and 3 K for the 4.6, 2.7, 1.7, 1.4, and 0.8 cm channels, respectively. For cloudliness, an error of 0.01 cm of cloud droplets in the column could lead to errors of about 0.5, 1.2, 3.5, 5, and 12 K for those five wavelengths. However, these potential errors are minimized by the adjustment procedure utilizing the observed minimum histogram values as described in Section 5.

The climatic values used for the first iteration on Equation 8 are SST=290.4 K, NSW=7 m/s, water vapor, w=1.6 cm, and weighted average atmospheric temperature=278.3 K. (A 10% error on this last factor would have negligible effect on the atmospheric contributions.) In the absence of any valid estimate of cloudiness, this parameter was set to 0, counting on the second-step adjustment to compensate for this shortcoming. For calculating the radiances corresponding to the histogram minima, the above parameters were changed to NSW=0 m/s, and w=1.0 cm. Selection of that value for w was based both on 1) a reasonable climatic value for the minimum water vapor in the zone and 2) matching the modeled and observed spectra of the water vapor contributions to the radiances by varying the value of w.

APPENDIX B.
PROGRAM LISTING FOR THE OCEAN/ATMOSPHERE RTE.
(written in Commodore Basic 7.0)

```
 1 rem *** o/a tb's 11 19 84 *** (uses wind coefficients from NOAA
buoys)
 10 s$="":i=0:ts=0:ta=0:ns=0:l=0:w=0:n=0:tv=0:tl=0:ox=0:tu=0:b0=0:
b1=0:b2=0:b3=0
 20 b4=0:b5=0:tb=0:z=0:q$="":pr=0:gr=0:gw=0:gt=0:c$=chr$(13)
 100 dim tb(4,10),a0(10),a1(10),a2(10),e0(10),de(10),f$(10),tu(5)
 105 dim a(10),b(10)
 110 print"this program is called 'o/a tb's 111984 (nsw coef.from
noaa buoys)'"
 135 rem**2nd-order fit of calculated ocean emissivities vs
temperature-kelvins*
 140 for i=1 to 10:read a0(i),a1(i),a2(i):next
 150 data 1.6143,-9.4331e-03,1.6377e-05,1.8500,-9.3437e-
03,1.6313e-05
 160 data 1.9026,-.01111,1.8824e-05,3.182,-.018025,3.0574e-05
 170 data 3.0135,-.01800,2.9603e-05,4.2522,-.024269,3.971e-05
 180 data 3.3311,-.01992,3.2531e-05,4.7888,-.02758,4.4896e-05
 190 data 4.2068,-.02464,3.8928e-05,5.0523,-.02774,4.3016e-05
 210 rem **emissivity for sst**
 220 for i=1 to 10:read e0(i):next
 230 data .25827,.51537,.27740,.54449,.31022,.59257,.32323,.61093,
.38804,.69502
 240 print"program to compute sea surface tb's based on pg's rte
model":print:print:print
 241 rem **channel wavelengths**
 242 data 4.6,4.6,2.8,2.8,1.7,1.7,1.4,1.4,.81,.81
 243 for i=1 to 10:read lamda(i):next
 244 rem **nsw coefficient (kelvins/meters per second)**
 245 gosub 2230
 250 open 1,4,1:open2,4,2:open3,4,0
 260 l$="         wind  vapor  sst   cloud    tb       pr      gr
gw     gt"
 270 f$="          zz     z    999   z.99    999.9  z.999 sz.999
sz.999 sz.999"
 280 print#2,f$
 290 print#3,l$:print#3:print#3
 291 rem***these loops automatically input the o/a parameters***
 292 for s=0to2:for w=0to8 step2:for ts=271to306 step5:for li=0to8
step2
 294 ta=ts-13:nsw=6^s:l=.01*li:if nsw=1 then nsw=0
 299 rem *** this computes temperature change in emissivity ***
 300 for i=1 to 10
 310 de(i)=a1(i)*(ts-271)+a2(i)*(ts^2-271^2)
 320 next
 330 for i=1 to 10
 340 e1(i)=e0(i)+de(i)
 360 next
 450 for i=1 to 10
 454 rem"The following is to compensate for the 2nd order curve
fit reversals"
 455 if i/2=int(i/2) and nsw<8 then nsw=8
```

```
 456 if i=5 and nsw<4 then nsw=4
 460 e1(i)=e1(i)+(b(i)/291*nsw)+(a(i)/291*nsw^2):rem**emisivity
changefrom nsw**
 465 nsw=6^s: if nsw=1 then nsw=0:rem***reset nsw for next loop***
 470 next
 480 n=z+1
 490 rem **tau from water vapor (source--ttw's/atcc's atmos.
prog.on 360)**
 500 if n=1 or n=2 then tv=1.05e-03*w+.04e-03
 505 if n=3 or n=4 then tv=3.10e-03*w+.10e-03
 510 if n=5 or n=6 then tv=1.94e-02*w+.03e-02
 515 if n=7 or n=8 then tv=6.78e-02*w+.05e-02
 520 if n=9 or n=10 then tv=3.29e-02*w+.12e-02
 590 rem **tau from cloud water (same source)**
 600 tl=2.61*l/lamda(n)^2
 601 rem**the following are oxygen line contributions:**
 602 if n=1 or n=2 then ox=3.8/ta
 603 if n=3 or n=4 then ox=3.9/ta
 604 if n=5 or n=6 then ox=4.5/ta
 605 if n=7 or n=8 then ox=4.8/ta
 606 if n=9 or n=10 then ox=13.4/ta
 610 tu=tv+tl+ox:if int(n/2)=n/2 then tu(n/2)=tu
 630 b1=e1(n)*ts*exp(-tu):rem **surface contribution**
 640 b2=(1-exp(-tu))*ta:rem **upwelling atmosperic contribution**
 650 b3=(1-e1(n))*(1-exp(-tu))*ta*exp(-tu):rem **downwelling atmos
contrib.**
 660 b4=(1-e1(n))*2.7*exp(-2*tu):rem **space contribution**
 680 tb=b1+b2+b3+b4
 690 tb(1,n)=b0
 700 tb(2,n)=b5
 710 tb(3,n)=b2+b3
 720 tb(4,n)=tb
 730 z=z+1
 740 if z>9 then 754
 750 goto 480
 754 z=0
 755 pr=(tb(4,4)-tb(4,3))/(tb(4,4)+tb(4,3))
 756 gr=(tb(4,10)-tb(4,6))/(tb(4,10)+tb(4,6))
 757 gw=(tb(4,8)-tb(4,6))/(tb(4,8)+tb(4,6))
 758 gt=(tb(4,10)-tb(4,4))/(tb(4,10)+tb(4,4))
 760 print#1,nsw,w,ts,l,tb(4,2),pr,gr,gw,gt
 762 next li:print#3:next ts:print#3:next w:print#3:next s
 763 rem ** only channel 2 (4.6V) radiances are printed out here,
but all others have been calculated and could be listed as tb(4,k)
where k=1 to 10**
 1010 print:print:restore:i=0:n=0:z=0:close1:close2:close3:
 2000 rem ** the following subroutine reads in data for the
coefficients used in line 460
 2230 rem **nsw coefficient (kelvins/meters per second)**
 2240 for i=1 to 10:read b(i):next
 2250 data .19932,-.16313,.29446,-.12915,-.12660,-.13174,-.12660,
-.13174
 2260 data .17995,-.08157
 2270 for i=1 to 10:read a(i):next
```

NASA
National Aeronautics and Space Administration

Report Documentation Page

1. Report No.	2. Government Accession No.	3. Recipient's Catalog No.
NASA TM-100678		

4. Title and Subtitle	5. Report Date
In-Orbit Calibration Adjustment of the Nimbus-7 SMMR	July 1987
	6. Performing Organization Code: 671.0

7. Author(s)	8. Performing Organization Report No.
Per Gloersen	87B0413
	10. Work Unit No.

9. Performing Organization Name and Address	11. Contract or Grant No.
Goddard Space Flight Center Greenbelt, Maryland 20771	
	13. Type of Report and Period Covered: Technical Memorandum

12. Sponsoring Agency Name and Address	14. Sponsoring Agency Code
National Aeronautics and Space Administration Washington, D.C. 20546-0001	

15. Supplementary Notes

16. Abstract

The procedure for converting raw antenna signals (counts) from the Nimbus-7 Scanning Multichannel Microwave Radiometer (SMMR) to microwave radiances is described. The procedure entails taking the raw data stored on TAT data tapes, applying an interim prelaunch calibration, correcting for polarization mixing, and finally adjusting the calibration so that the observations conform to model calculations of oceanic radiances. The results are stored on TCT data tapes with the same format as the TATs, i.e., the basic sampling interval of the SMMR is retained. The properties of the TCTs are compared with those of the other basic SMMR radiance data product, the CELL tapes, in which the integrated fields-of-view (IFOVs) have been averaged into cells with coarser sampling intervals and in which the prelaunch calibration is the final one used.

17. Key Words (Suggested by Author(s))	18. Distribution Statement
Nimbus-7; Passive Microwave; Calibration Adjustment; SMMR	Unclassified - Unlimited Subject Category 42

19. Security Classif. (of this report)	20. Security Classif. (of this page)	21. No. of pages	22. Price
Unclassified	Unclassified		